MQP-BIO-DSA-8933
MQP-BC-DSA-1773

ROLE OF SOD AND CATHEPSIN-D IN ALZHEIMER'S DISEASE Aβ CASCADE MODELS

A Major Qualifying Project Report

Submitted to the Faculty of the

WORCESTER POLYTECHNIC INSTITUTE

in partial fulfillment of the requirements for the

Degree of Bachelor of Science

in

Biology and Biotechnology (MD)

and

Biochemistry (GL)

by

Melanie K. Donahue

Gregory Lobdell

April 28, 2011

APPROVED:

David S. Adams, Ph.D.
Biology and Biotechnology
Major Advisor
WPI Project Advisor

ABSTRACT

Alzheimer's disease (AD) is thought to be initiated by the formation of extracellular amyloid-β (Aβ) neurotoxin. Our laboratory uses neurotrophic factor (NTF) mimetics to increase neuronal survival in the presence of Aβ. This project investigated the potential role of the lysosomal protease cathepsin-D (Cat-D) in Aβ-induced cell death *in vitro*, and the effect of NTF therapy on cellular levels of therapeutic anti-oxidative superoxide dismutase (SOD) *in vivo.* A fluorescence substrate assay demonstrated that Cat-D activity increases in Aβ-treated human neuronal SHSY cells, while immunoblots demonstrated that NTF treatment increases the cellular levels of SOD in the brains of AD mice. Cell morphology and viability counts demonstrated that NTF treatment restores viability and neuronal connections *in vitro*, and thus may rescue Cat-D activity levels, as well. Further testing will be required to determine this effect of NTF on Cat-D activity, and accurately place Cat-D within the hypothesized cell death cascade.

ACKNOWLEDGEMENTS

We would first and foremost like to extend our sincerest gratitude to our project advisor, Dr. Dave Adams. His expertise and genuine enthusiasm in the field of Alzheimer's disease has not only been an asset to our project's planning and execution, but an inspiration for our own intense interest in our work. Further, his continuous support and guidance throughout the project enabled us not only to complete important preliminary investigations of novel features in Alzheimer's disease pathways, but to grow as both scientists and critically thinking members of society.

We would also like to thank Dr. Daniel Raimunda (Postdoctoral Fellow, Arguello lab) for providing the initial training on the Gateway Photon Technology International (PTI) fluorimeter and software, as well as two former graduate students in our lab (Varun Kapoor and Devika Rawal) for the frozen SHSY-5Y cell stocks used in our *in vitro* model experiments. Finally, we would like to thank BioTherapeutix, Inc. (Belmont, MA) for their aid in financially supporting this work.

TABLE OF CONTENTS

BACKGROUND

Alzheimer's Disease

Introduction

Alzheimer's disease (AD) was first characterized over a century ago in a single patient of the German physician Dr. Alois Alzheimer (Alzheimer's Foundation, 2010). Today, AD is the underlying neurodegenerative disorder responsible for the largest percentage of dementia cases worldwide, including an estimated 60 and 80% of all documented cases in the United States (AD Association, 2010; Alzheimer's Foundation of America, 2010). With another American predicted to develop AD every 70 seconds (AD Association, 2010), and this rate is forecast to rise with increasing life expectancies, the disease has recently been repositioned at the forefront of both therapeutic and preventative research initiatives to control its widespread medical, social, and economic repercussions.

Symptoms

Early symptoms of AD include impaired functioning in basic tasks and short term memory retention, particularly in recalling names and recent events, as well as psychological modifications such as general apathy or depression (Alzheimer's Association, 2010) due to the concentrated neuronal cell death in the hippocampus and entorhinnal cortex (Progress Report, 2009; Alzheimer's Foundation of America, 2010). As the disease progresses, compromising surrounding regions of the brain, the initial memory loss, disorientation, confusion, and psychological effects become more severe while symptoms extend to further cognitive functions including judgment, behavior, speaking, swallowing, and motor control (Alzheimer's Foundation of America, 2010; Progress Report, 2009; Alzheimer's Association, 2010). Accompanying sensory decline, such as that shown in visuo-spatial (Johnson *et al.*,

2009) and olfactory (Wilson *et al.*, 2009) systems, may even lead to hallucinations (Alzheimer's Foundation of America, 2010), completing the "Four A's" of Alzheimer's – amnesia, aphasia, apraxia, and agnosia (AFA, 2010). Although these symptoms typically appear between age 60 and 70, early-onset cases occur more rarely with symptoms first appearing in the 40's and 50's. The latter cases typically have a genetic component, and are termed Familial AD (FAD).

At the cellular level, patients generally present several pathological anomalies hallmark to AD, including extracellular aggregations of beta-amyloid (Aβ) protein fragments known as "plaques", intracellular interwoven fibers of abnormal hyper-phosphorylated tau protein known as "neurofibrillary tangles", and general brain atrophy due to the neuronal death caused by widespread synaptic disruption (Alzheimer's Association, 2010; Progress Report, 2009; AFA, 2010). The average life span following AD diagnosis is 8 to 10 years, at which point complications such as immobility and difficulty swallowing often lead to fatal pneumonia (Alzheimer's Association, 2010). **Figure-1** outlines these stages of AD from pre-symptomatic through advanced dementia relative to various bio-markers.

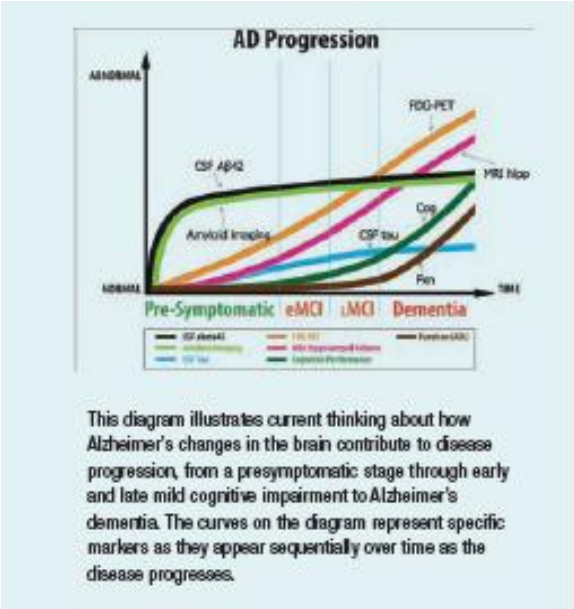

Figure-1: Diagram of the Various Stages of AD. Shown are the stages of AD from early pre-symptomatic through advanced dementia relative to several hallmark bio-markers. (Progress Report, 2009)

Figure-2 displays cross-sectional views of a normal human brain (upper) and an advanced AD brain (lower), clearly illustrating the severe tissue damage in the temporal lobes and an expansion of the central ventricles.

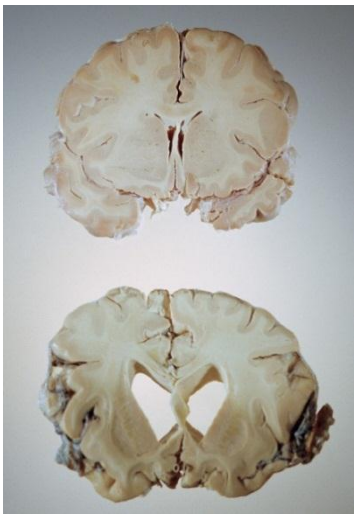

Figure-2: Photographs of Normal Human Brain (Upper) and AD Brain (Lower). (Sanders, 2011)

AD Diagnosis

Alzheimer's disease is traditionally diagnosed by a combination of observable behavioral changes, individual and familial medical histories, cognitive function assessments, and periodic brain imaging. However, at present, experienced physicians are capable of discerning symptomatic "Possible AD" dementia (a diagnosis which leaves the potential for an alternate cause) and "Probable AD" dementia (with no apparent alternate cause) from other neurological disorders with approximately 90% accuracy (Progress Report, 2009), at which point 60 to 70% of the neurons in the brain are likely already damaged or dead (Sanders, 2011). AD may only be conclusively diagnosed by the presence of Aβ plaque and neurofibrillary tau tangle pathologies in a postmortem autopsy (Progress Report, 2009; AFA, 2010).

More advanced diagnostic protocols for enhanced sensitivity to early AD and discrimination between types of dementia are currently under investigation in order to promote early preventative treatment and reduce neuronal loss. Standard dementia tests dating back to the 1970's, such as the Mini Mental State Examination (MMSE), are undergoing modernization to be self-administered and computer-scored (Saxton *et al.,* 2009). Brain imaging initiatives, such as the Alzheimer's Disease Neuroimaging Initiative (ADNI) launched in 2004, are investigating biomarkers and scan features unique to AD (Progress Report, 2009), while improved PET imaging using florbetapir has been shown to accurately predict up to 96% of AD cases according to validation by postmortem autopsy (Clark *et al.,* 2011). Further, Aβ plasma levels have been negatively correlated with cognitive decline in a sample of non-dementia elderly, suggesting that as the AD brain forms Aβ-containing senile plaques less Aβ is free to move to the plasma, thus diminishing plasma levels and in turn implicating the diagnostic potential of simple blood tests (Yaffe *et al.,* 2011).

AD Risk Factors

Age is currently the leading risk factor for the development of AD. Upwards of 90% of diagnosed AD individuals are age 60 or older, and the number of individuals within this population doubles for every five year interval beyond age 65 (Progress Report, 2009). Though the precise relationship between age and the development of AD remains murky, the decline in mitochondrial function and metabolic shift of neurons from glucose to fats and amino acids which occurs normally in aging has been suggested to predispose the brain to AD (Yao *et al.*, 2009; Kadish *et al.*, 2009). In addition, any decline in the brain's normal ability to prevent Aβ build-up (i.e. a decline it its ability to remove Aβ) would lead to increased brain levels of the toxin (Mawuenyega *et al*., 2010).

Genetics has also been shown to play a major role in AD development. Mutations in three particular genes, amyloid precursor protein (APP) of chromosome-21, presenilin-1 of chromosome-14, and presenilin-2 of chromosome-1, have been strongly associated with the increased processing of APP protein to form toxic Aβ in early-onset familial AD (Progress Report, 2009). In addition, the ε4 allele of a fourth gene, apolipoprotein E (apoE) on chromosome-19, has also been named as a major genetic risk factor in late-onset, sporadic AD (Roberson & Mucke, 2006), and the copy number of this ε4 allele has been positively correlated with high aggregate Aβ loads in the cortical, frontal, temporal, posterior congulate-precuneus, parietal, and basal ganglia of human brains by Pittsburg Compound B (PiB) PET scans (Reiman *et al.*, 2009). Several other genes, including cluserin (apoJ, or CLU), phosphatidylinositol-binding clathrin assembly protein (PI CALM), CR1, and ADAM10, have also been implicated by the Genome-Wide Association Study (GWAS) and smaller projects in the development of late-onset AD (Harold *et al.*, 2009; Progress Report, 2009).

Due to the largely unknown mechanism of AD pathology, a variety of other conditions have also been suggested as risk factors for the disease. Various epigenetic case

studies offer a variety of "nature-nurture" scenarios, such as the recent implications in one twin study of lowered DNA methylation due to pesticide exposure (Mastroeni *et al.,* 2009). Other research suggests that vascular disease, diabetes, Lewy body disorders, and other conditions common in aged populations may increase AD susceptibility (Schneider *et al.,* 2009; Sonnen *et al.,* 2009). Also implicated are sleep deprivation, hormone imbalances, anesthetics, toxic free radicals, brain injuries, and general inflammation (Dong *et al.,* 2009; Kang *et al.,* 2009; AFA, 2010). Much research in preventative measures to counter some of these risk factors has also been conducted, which suggests that ample social interaction, healthy diet and exercise, mental exercise, and engaging in "enriching life experiences" might act as neuroprotective practices to combat AD (Carlson *et al.,* 2009; Progress Report, 2009; Smith *et al.,* 2009).

AD Prevalence

As of 2009, an estimated 5.1 million Americans are reported to suffer from AD, including one of every eight individuals age 65 or older (**Figure-3**) (Progress Report, 2009; AFA, 2010; Alzheimer's Association, 2010). Worse, these numbers are definitively increasing due to better diagnostic tools and increased life expectancy, with forecasts to nearly double as soon as 2030 (Alzheimer's Disease International, 2010). Incidence rates are higher in women than men and in African American and Hispanic populations than Caucasian while also varying hugely between global regions, most likely due to differential gender life expectancies, medical reporting infrastructure, disease recognition, population genetics, or other demographical risk factors (Alzheimer's Association, 2010).

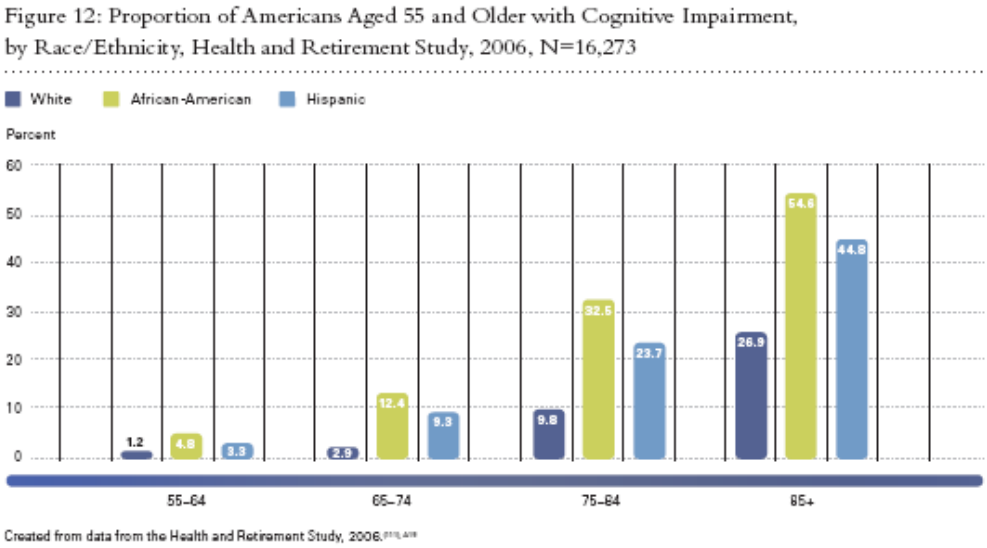

Figure-3: Alzheimer's Disease Cognitive Impairment for Various Age Groups. (Alzheimer's Association, 2010)

Due to this high prevalence, AD was found to be the sixth leading cause of death in the United States in 2006, and fifth among those 65 and older (Alzheimer's Association, 2010), surpassing diabetes from the previous year (Heron *et al.*, 2008). Further, while mortality rates from other leading causes of deaths worldwide decreased between 2000 and 2006, including those of stroke, cancer, and the highest ranking heart disease, AD deaths increased by 46.1% (Alzheimer's Association, 2010).

AD Therapies

The search for AD therapies is supported by a wide base of both national and international platforms, including the NIA Division of Neuroscience Translational Research Platform and Alzheimer's Disease Centers, National Alzheimer's Coordinating Center, National Cell Repository for Alzheimer's Disease, and the Genetics of Alzheimer's Disease Data Storage Site (Petanceska *et al.*, 2009; Alzheimer's Association, 2010). Though no cure currently exists for AD, five FDA approved drugs and approximately 90 experimental

courses of therapy are in use in the U.S. in attempts to slow or stop the progression of the disease (Alzheimer's Association, 2010). Of the five approved medications, cholinesterase inhibitors (donepezil, galantamine, rivastigmine, and tacrine) attempt to offset damage to cholinergic neurons in AD by inhibiting the enzymatic degradation of synaptic acetylcholine, while the fifth medication (memantine) prevents excitotoxic overstimulation of NMDA glutamate receptors (Roberson & Mucke, 2006). These two AD therapy regimens are often used together, though their effects target the symptoms rather than the source of AD.

Other treatments approved for non-AD disorders, such as antipsychotics, anti-depressants, nonsteroidal anti-inflammatory drugs (NSAIDS), sildenafil (Viagra®), and immune-modulatory polypeptide glatiramer (used in multiple sclerosis), have also been tested in AD cases based on their applications to the documented symptoms (Roberson & Mucke, 2006; Puzzo *et al.,* 2009). Clinical trials have also investigated correlations between AD and factors such as depression, sleep apnea, and the consumption of gingko biloba, DHA omega-3 fatty acids, and resveratrol (Lu *et al.,* 2009a; Cooke *et al.,* 2009; Snitz *et al.,* 2009; Progress Report, 2009, page 42).

Recently, novel experimental treatment approaches for AD have focused on preventing the formation of toxic Aβ by blocking gamma and beta-secretases, blocking apoptotic caspases, removing toxic Aβ from the brain through immunizations, upregulating Aβ transport proteins, prohibiting the aggregation of Aβ, and inhibiting the hyper-phosphorylation and aggregation of tau protein (Roberson & Mucke, 2006; Kim *et al.,* 2009; Lu *et al.,* 2009b; Luo *et al.,* 2010). Among these novel therapies is the elevation of nerve growth factor (NGF) levels in the brain, stimulating the replacement of damaged or dead neurons (Roberson & Mucke, 2006; Progress Report, 2009), a neuroregenerative approach our lab initially applied to brain ischemia (Adams *et al*., 2003; Shashoua *et al*., 2003) and is currently testing for AD.

AD Socioeconomic Toll

According to the CDC World Alzheimer's Report, released in 2001:

> "If dementia care was a country, it would be the world's 18th largest economy, ranking between Turkey and Indonesia. If it was a company, it would be the world's largest by annual revenue, exceeding Wal-Mart (US $414 billion) and Exxon Mobil (US $311 billion)" (Vas, 2001).

In our country alone, the national tab for AD care is estimated to exceed $100 billion annually, including $60 billion lost solely to companies and corporations through decreased productivity of caregivers and insurance fees (AFA, 2010; Alzheimer's Association, 2010). These numbers also do not account for the time and energy donated by the approximately 10.9 million emotionally stressed and unpaid caregivers and family members, estimated at an additional $144 billion (**Figure-4**). These soaring expenditures are a result of the substantial percentage of all medical attention which the elderly, and particularly those with dementia, require – as 12% of the population, they constitute 20% of physician visits, 30% of prescriptions, 30% of all hospital visits, 40% of emergency responses, and 90% of nursing home residents (Alzheimer's Association, 2010). As the average population ages, and the incidence rate of AD increases, so will these monetary and emotional tolls.

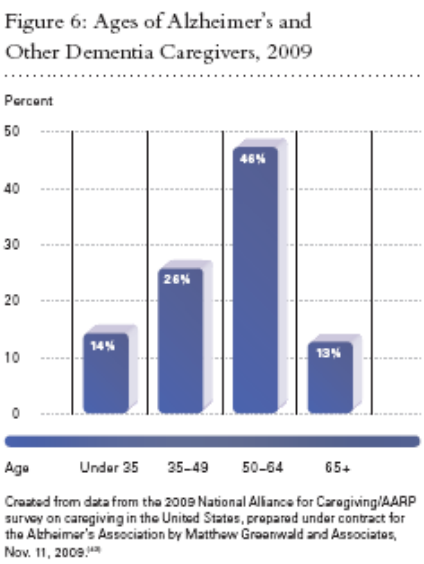

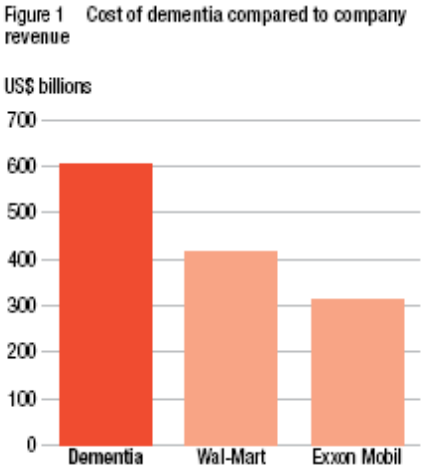

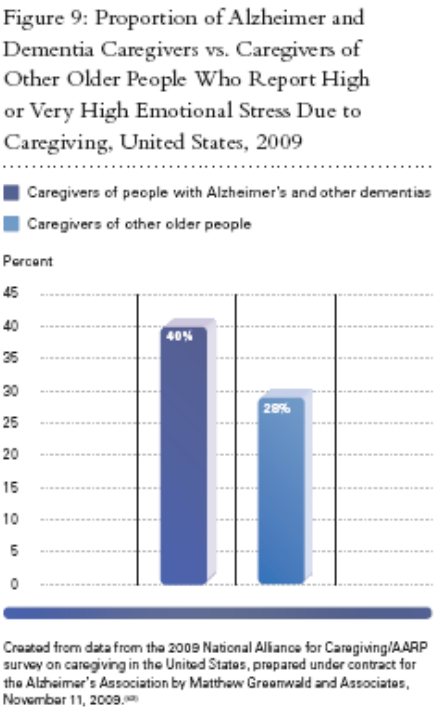

Figure-4: Cost of AD Dementia and Statistics on Caregivers. (Alzheimer's Association, 2010)

AD Cellular Pathology and the Amyloid Cascade Hypothesis

The hallmark AD extracellular senile plaques and intracellular neurofibrillary tangles originally seen by Alois Alzheimer nearly a century ago have been diagnostic in AD

neuropathology ever since. However, the precise mechanism of AD continues to remain a mystery. Over time research has identified several key mechanistic theories to explain its initiation and progression, which are now dominated by the favored amyloid cascade hypothesis (**Figure-5**). According to this mechanistic explanation for AD, pathogenesis begins with the generation of the 40 or 42 amino acid amyloid-beta peptide (Aβ) by genetic defect or abnormal processing of the 770 amino acid amyloid precursor protein (APP) via gamma- and beta-secretases (Armstrong, 2006; Verdile *et al*., 2004; Goedert and Spillantini, 2006; Zheng and Koo, 2006). Analysis of peptide levels in AD brains implicate the soluble AB_{42} variant as the most pathogenic form of the protein fragment and the key player in the initiation of the cascade (Yuan and Yankner, 2000; Takahashi *et al*., 2008). These soluble, highly neurotoxic protein fragments aggregate over time to form extracellular oligomers and, eventually, the disease's hallmark senile plaques. Although these senile plaques have long been held accountable for the disruption of synapse-strengthening long term potentiation (LTP), induction of oxidative stress, and intracellular accumulation of altered tau protein (Progress Report, 2009; Walsh *et al.*, 2002), recent experiments indicate that low molecular weight Aβ monomers and dimers are far more toxic. In particular, these forms of Aβ have been shown to achieve their toxic effects by activating, both directly and indirectly, key receptors for oxidative stress induction and intracellular death signal stimulation through receptors such as RAGE and TNF-R (Yan *et al*., 1996; Yuan and Yankner, 2000). Thus new drug discovery initiatives to alleviate Aβ-induced cell death must block both apoptotic and oxidative stress pathways.

The amyloid cascade hypothesis has been challenged as an accurate model of AD initiation and pathogenesis, particularly due to the discovery of significant Aβ loads in non-demented individuals, the absence of such loads in demented individuals, and null correlation between plaque clearance and rescued cognitive function (Sanders, 2011). Models placing

inflammation, neuronal DNA duplication, and neurofibrillary tau tangles at the forefront of AD pathology have been offered as alternatives (Rapoport *et al*., 2002; Verdile, 2004; Sanders, 2011). However, mutagenesis experiments have brought the Aβ cascade and tau models together to show that abnormal tau production occurs downstream from the Aβ initiation of cell death, and is required for one of the end stages of death as neurons lose their characteristic shape (Rapoport *et al*., 2002; Roberson *et al*., 2007). Other "theory merging" findings include the post-synaptic co-localization of $A\beta_{42}$ and tau, the direct impact of Aβ and anti-Aβ introduction on tau pathology, and the sequestering of the signaling molecule EphB2 by Aβ, causing severe AD-like cognitive impairment (Sanders, 2011). Thus, despite scrutiny from the scientific community, substantial support for the amyloid cascade continues to bolster its acclaim.

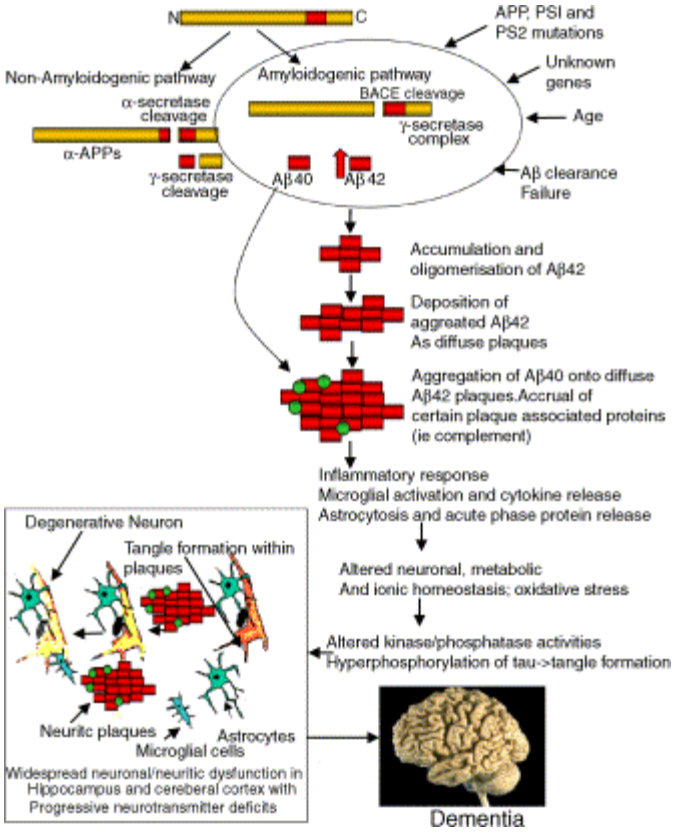

Figure-5: The Amyloid Cascade Hypothesis. The amyloid cascade hypothesis states that Aβ is the major cause for neuronal death and dysfunction in AD dementia. Genetic and environmental influences (i.e. APP, PS1 and PS2 mutations) cause a dysregulation in APP processing resulting in an over-production and accumulation of highly neurotoxic $A\beta_{42}$ peptide leading to diffuse plaque deposition. Abnormal cell signaling leads to abnormal tau production and synaptic loss. The formation of these plaques results in microglial and astrocytic activation, oxidative damage, and tau aggregation culminating in neuronal loss leading to dementia. (Verdile *et al.*, 2004)

Neurotrophic Factors

Neurotrophic factors (NTFs) are proteins that function in nerve regeneration, synaptic outgrowth, and long-term memory consolidation in the brain (Lindsay *et al.*, 1994; Progress Report, 2009). NTF levels increase in the brain post-injury (Connor and Dragunow, 1998; Ferrer *et al.*, 1998) while gene therapy and stem cell techniques boosting NTFs have demonstrated rescue of impaired synaptic function and memory (Nagahara *et al.*, 2009; Blurton-Jones *et al.*, 2009). Therefore, NTFs have been studied as possible therapeutics for

brain-related neurological disorders such as AD (Barinaga, 1994; Tuszynski and Gage, 1994; Shen *et al.,* 1997; Hefti, 1997; Yu and Silva, 2008; Zuccato and Cattaneo, 2009).

Ependymin (EPN) is a glycoprotein NTF first discovered in the *zona ependymal* cells of goldfish brain (Benowitz and Shashoua, 1997). Subsequently, ependymins were characterized in other organisms, including mice, monkeys, and humans (Adams and Shashoua, 1994; Adams *et al*., 1996; Apostolopoulos *et al*., 2001). EPN was pursued by our lab as an attractive candidate for an Alzheimer's disease NTF therapeutic, however full-length NTFs are difficult to deliver to the brain due to their inefficient crossing of the blood brain barrier (BBB), leaving surgical intra-cranial injection as the only mode of delivery. To avoid surgical delivery, our laboratory is developing a therapeutic approach using shorter synthetic versions of EPN, called EPN peptides, which more efficiently cross the BBB. Using this peptide approach, our lab previously demonstrated that treating cultured human SHSY cells with $A\beta_{25-35}$ decreases cell survival, while the addition of human EPN-1 peptide (hEPN-1) can restore cell survival (Stovall, 2006).

Cathepsin-D

The lysosomal cysteine proteases known as cathepsins are the largest cohort of proteolytic lysosomal enzymes, comprised of eleven known varieties – B, H, L, S, F, K, C, W, X, V, O – plus the lone aspartic lysosomal protease cathepsin-D (Cat-D) (Guicciardi *et al*., 2004; Chwieralski *et al*., 2006). Cathepsins B, L, and D, are ubiquitously expressed and found in the greatest quantities throughout the body (Guicciardi *et al.*, 2004). All cathepsins in the inactive pro-enzyme form are processed to catalytically active proteases in the acidic environment of the lysosome, where they were traditionally believed to exist solely for protein degradation and debris clearance from the cell. However, recent research has illuminated other functional roles for cathepsins in a variety of pathways, ranging from

protein processing and antigen recognition (cathepsin-B), to antigen presentation (cathepsin-L, S), to bone remodeling (cathepsin-K), to protein targeting and neurodegenerative apoptosis (cathepsin-D) (Guicciardi *et al.*, 2004; Chwieralski *et al.*, 2006). Some roles describe the release of these proteases from the acidic lysosomes to the neutral cytosol by lysosomal permeabilization, a process thought to be initiated by factors such as TNF-α and excess free Ca^{2+} which precedes caspase activation and mitochondrial dysfunction *in vitro* (Bidere *et al.*, 2003; Chwieralski, 2006).

Of the twelve known cathepsins, this project focused on the aspartic protease Cat-D. This cathepsin is known to affect tissue homeostasis in post-natal humans and has been shown to stimulate metastasis in some cancers (Benes *et al.*, 2008). Cat-D has also been implicated in cancer and neurodegenerative apoptotic pathways induced by factors such as staurosporine, sphingosine, interferon-γ, and FAS/CD95/APO-1, as well as TNF-α and oxidative stress, which play pivotal roles in AD pathogenesis (Guicciardi *et al.*, 2004). However, the precise role of Cat-D in apoptotic pathways is not yet known. Scattered reports indicate Cat-D plays a cell death role by increasing the activity of caspases, increasing ROS, and decreasing mitochondrial function (Vancompernolle *et al.*, 1998; Zhao *et al.*, 2003; Bidere *et al.*, 2003; Conus *et al.*, 2008). Polymorphisms in the Cat-D gene have also been loosely correlated with an increased risk for sporadic AD (Papassotiropoulos *et al.*, 1999; Shuur *et al.*, 2009), and Cat-D activity has been shown to increase early in AD (Cataldo *et al.*, 1995). Yet other studies alternately indicate a positive role for Cat-D in the degradation of toxic protein accumulations *in vivo*, such as the alpha-synuclein, $A\beta_{42}$, and tau aggregations which encompass the hallmark pathologies of Lewy Body and AD dementia (Qiao *et al.*, 2008; Leissring *et al.*, 2009). Thus, while research has established Cat-D within a selection of AD-associated pathways, it remains unclear whether Cat-D plays an aggravating or restorative role in AD neuronal apoptosis.

Superoxide Dismutase (SOD)

Anaerobic cells produce reactive oxygen species (ROS) which are believed to contribute to the aging process and many neurodegenerative diseases (Venarucci *et al*., 1999; Allen and Tresini, 2000). The accumulation of ROS triggers oxidative stress which causes cellular damage and eventually cell death. Aβ has been shown to increase the expression of Hemoxygenase type 1 (HO-1) and cellular oxidative stress in SHSY cells (Yan *et al*., 1996). Superoxide dismutase (SOD) is an anti-oxidative enzyme which catalyzes the dismutation of anionic superoxide in the presence of molecular hydrogen to molecular oxygen and hydrogen peroxide (**Figure-6**; Venarucci *et al*., 1999; Allen and Tresini, 2000).

$$O_2^- + O_2^- + 2\,H^+ \xrightarrow{SOD} H_2O_2 + O_2$$

Figure-6: Chemical formula for the dismutation of anionic superoxide, catalyzed by SOD.

SOD primarily acts to protect oxygen-metabolizing eukaryotic cells from the detrimental effects of superoxide free radicals (McCord *et al.*, 1971). Transgenic flies overexpressing SOD show a decreased level of oxidative damage and a 33% increase in life-span compared to the diploid controls (Orr and Sohal, 1994). Also, transgenic mice exhibiting diminished SOD expression show an increased predisposition to stroke (Sheng *et al*., 1999; Sampei *et al*., 2000). Previous work in our lab showed that the treatment of cultured mouse neuroblastoma cells *in vitro* with a goldfish ependymin mimetic (CMX-8933) increased the expression of SOD-1 (Parikh, 2003) which may in turn help to alleviate Aβ-induced oxidative stress in neuronal cells. This project will test the effects of a human NTF hEPN on this therapeutic enzyme in transgenic AD mice.

PROJECT PURPOSE

This project will investigate the potential role of the lysosomal protease cathepsin-D (Cat-D) in Aβ-induced cell death *in vitro,* and the effect of NTF therapy on cellular levels of therapeutic anti-oxidative superoxide dismutase (SOD) *in vivo.*

Although Cat-D has previously been implicated in AD, the literature is conflicting; some studies indicate Cat-D induces neuronal apoptosis by activating caspases and increasing ROS, while other studies suggest a neuroprotective role through the degradation of toxic proteins similar to Aβ. A fluorescence substrate assay will be used to measure Cat-D activity in Aβ-treated human neuronal SHSY cells, and to determine whether altered activity levels are rescued following treatment with neurotrophic factor. Cell morphology and viability counts will also be monitored during the Aβ and NTF treatments.

Alternately, ROS has been shown to play a direct role in neuronal death due to AD. Because SOD is an enzyme known to therapeutically reduce ROS, we will also investigate whether our neurotrophic factor treatment could increase the cellular levels of SOD in the brain. These SOD levels in AD transgenic mice treated with vehicle or NTF will be measured by immunoblot analysis.

MATERIALS AND METHODS

In vivo AD Mouse Model

Alzheimer's mice (5X transgenic for human amyloid precursor protein (APP) and presenilin (PSEN) mutations; The Jackson Laboratory #006554) were aged to 9 months, at which age senile plaque formation is prevalent, then dosed 2X per day for two weeks with 20 mg/kg hEPN NTF mimetic, after which brains and livers were harvested and stored at -80ºC.

Genotyping AD Mouse Tissues

Genotypes of AD mice were confirmed through PCR for APP and PSEN transgenes. DNA was isolated by both crude alkaline tissue lysis and phenol extraction techniques, then amplified with primers for human APP or PSEN.

Alkaline Lysis of AD Mouse Liver

Isolated liver tissue from AD mice was retrieved from -80°C storage, and thawed for five minutes. A 2 mm liver section was cut using a razor blade, and placed in a 1.5 mL microfuge tube. A 75 µL aliquot of Lysis Buffer (25 mM NaOH, 0.2 mM EDTA) was added to each tissue section, and each tube was placed in a thermocycler at 98°C for one hour, then cooled to 15°C. Each tube was briefly micro-centrifuged to pull solution from the lid, then 75 µL of Neutralization Buffer (40 mM Tris-HCl, pH 5.5) was added to each tube and mixed by inversion. Each sample was then centrifuged at 4000 rpm for three minutes to pellet cell debris. A 10 µL aliquot of supernatant was taken to be used later in PCR, and the remaining lysate was stored at 4ºC.

PCR

Master mixes (400 µL) were prepared for ten APP and PSEN genotyping reactions (50 µL per reaction) according to the following table:

APP: • 237 µL of dH_2O • 50 µL of 10X PCR buffer • 25 µL of 50 mM $MgCl_2$ • 10 µL of 10 mM dNTPs • 25 µL of 20 µM APP-3610 • 25 µL of 20 µM APP-3611 • 12.5 µL 20 µM Ctrl-8744 • 12.5 µL of 20 µM Ctrl-8745 • 3 µL of 5 U / µL Taq Polymerase	**PSEN**: • 196 µL of dH_2O • 50 µL of 10X PCR buffer • 25 µL of 50 mM $MgCl_2$ • 10 µL of 10 mM dNTPs • 33 µL of 20 µM PSEN-1644 • 33 µL of 20 µM PSEN-1645 • 25 µL 20 µM Ctrl-7338 • 25 µL of 20 µM Ctrl-7339 • 3 µL of 5 U / µL Taq Polymerase

Master mix (40 µL) was aliquoted into tubes containing 10 µL of tissue lysate (to make a 50 µL reaction), then subjected to PCR as follows: Step 1: 94°C for three minutes; Step 2: 94°C for 30 seconds, 52°C for one minute, 72°C for one minute; Repeat Step 2 for 35 cycles; Step 3: 72 °C for two minutes; Step 4: 4 °C infinitely. Following PCR, 5.5 µL of 10X Sample Buffer (0.025% xylene cyanole, 100 mM EDTA pH 8.0, 50% glycerol) was added to each 50 µL reaction, then 10 µL was loaded onto a 2.5% agarose gel in 1X TAE buffer containing 1 µg/mL (final concentration) Ethidium Bromide. The first lane was loaded with 10 µL of 100 bp DNA ladder (0.5 µg). Gels were electrophoresed at approximately 60 V for 1.5 hr, then were photographed by UV trans-illumination.

Brain Whole Cell Lysates

A small slice of brain tissue (0.1 mg) was mixed with 1 mL of Complete Lysis Buffer [20 mM HEPES pH 7.9, 10 mM KCl, 300 mM NaCl, 1 mM $MgCl_2$, 0.1% Triton X-100, 20% glycerol, 0.5 mM DTT (freshly added; Gibco), and 0.5 mM PMSF (freshly added; Sigma)],

then homogenized by ten up-and-down strokes using a 1 mL glass dounce homogenizer. Homogenates were incubated on ice for five minutes with occasional vortexing to ensure cell lysis, then microfuged for five minutes at 13,000 rpm to pellet cell debris. Supernatant aliquots were stored at -80°C.

SOD & Tubulin Immunoblots

Total cellular protein concentrations for each lysate were assayed by Bradford Assay. Appropriate volumes providing 5 µg per lane for tubulin or 2 µg per lane for SOD were mixed with 4X sample buffer (0.5 M stacking gel buffer, 8% SDS, 20% glycerol, 40% β-mercaptoethanol, and 0.4% bromophenyl blue) to make a total load volume of 5 µL. Kaleidoscope Pre-Stained Standard (10 µL, Bio-Rad) was mixed with an equal volume of 1X sample buffer (20 µL load volume). The Biotinylated Broad Range Standard (Bio-Rad) was prepared using 10 µL of 1X sample buffer and 1 µL (0.5 µg) of the biotinylated standard. All samples were boiled for two minutes to ensure protein denaturation, then loaded onto gels containing 10% polyacrylamide, 0.38 M resolving buffer, 0.1% SDS, 0.1% ammonium persulfate, and 0.05% TEMED. The upper stacker was composed of 5% polyacrylamide, 0.125 M stacking buffer, 0.1% SDS, 0.1% APS, 0.1% TEMED. Electrode buffer included 25 mM Tris, 0.192 M glycine, and 0.1% SDS. Gels were pre-run for five to ten minutes at 150 volts to equilibrate with the buffer, then electrophoresed for approximately 150 volts for three hours.

Once electrophoresis was complete, the protein was electroblotted to nitrocellulose membrane (Whatman, 0.45 µm pore size) in pre-chilled transfer buffer (48 mM Tris, 39 mM glycine, 0.037% SDS, 20% methanol). Transblotting was performed at 50 volts for two hours at 4°C with stirring. Membranes were then submerged in blocking solution (1%

casein, 1X PBS, 0.2% Tween- 20) with the membrane protein-side up. The membrane was blocked for at least one hour at room temperature with rocking.

Primary antibody incubations for SOD contained 25 μL of 90 mg/ml rabbit anti-bovine SOD-1 (Rockland) added to 50 mL of fresh blocker solution (1:2000 dilution), to give a final concentration of 45 μg/mL. Primary antibody incubations for β-tubulin contained 25 μL of 500 μg/ml anti-β-tubulin (Imgenex, IMG-5810A) mixed with 50 mL of fresh blocker solution (1:2000 dilution) to give a final concentration of 0.25 μg/mL. Membranes were incubated with primary antibody for two hours at room temperature with rocking, then were washed twice for two minutes with PBS-Tween (1X PBS, 0.05% Tween) using vigorous shaking on a gyratory shaker. Secondary antibody incubations included a 0.4 mg/mL final concentration of goat-anti-rabbit-HRP (Pierce) and a 0.5 mg/mL final concentration Streptavidin-HRP (Pierce; 1:1000 dilutions of glycerol stocks; 25 μL of secondary antibody added to 25 mL blocker). Secondary antibody incubations were performed for two hours at room temperature with gentle shaking. Membranes were then washed three times with PBS-Tween for two minutes with vigorous shaking on a gyratory shaker, then rinsed briefly with 1X PBS before detection.

SuperSignal West Pico chemiluminescent substrate (Pierce) was used to detect protein presence by combining equal amounts of Stable Peroxidase Solution and Luminol/Enhancer Solution just prior to use, and incubating the membrane in the fresh substrate solution for five minutes with protein-side facing upward at room temperature. The substrate was then allowed to drip from the membrane without drying, then placed between two clear plastic sheets (Gibco) in a film cassette. Tubulin blots were exposed to Biomax XAR-5 film (Kodak) for four minutes, and SOD blots for one second. Film was developed automatically in the Kodak M35A X-Omat Processor.

Human SH-SY5Y Cell Culture

Human SH-SY5Y neuroblastoma cells (commonly termed SHSY) were obtained from medium-adapted liquid nitrogen stocks previously prepared in our laboratory. Culture medium contained 500 mL DMEM-F-12 (ATCC), 50 mL of FBS (Gibco, ATCC, or Hyclone) to give a final concentration of 10%, and 0.275 mL of 10 mg/mL gentamycin (BioWhittaker) to give a final concentration of 5 μg/mL. The DMEM-F-12, FBS, and gentamycin were mixed in the 500 mL medium bottle, then filter sterilized. Medium was stored at 4°C.

To thaw our lab's SHSY cells from liquid nitrogen storage, the cells were placed in a 37°C water bath for one to two minutes until completely thawed, then carefully re-suspended and transferred into a 15 mL conical tube where 5 mL of pre-warmed medium was added. The tube was centrifuged for five minutes at 6500 rpm, the supernatant aspirated from the tube, and the cell pellet re-suspended in 4 mL of pre-warmed cell culture medium, which was then plated into a T-25 flask and placed in a 37°C + 5% CO_2 humidified incubator. We did note, however, that this protocol for thawing and plating appeared to damage commercially purchased ATCC vials of frozen cells.

Cultures were fed every 3-4 days until flasks achieved approximately 80% confluency, at which point cultures were split 1:2 into new flasks. To feed cultures, the old medium was aspirated and replaced with 4 mL of fresh, pre-warmed medium. To split cultures, the old medium was aspirated and replaced with pre-warmed medium (8 mL for T-25, 30 mL for T-75), and the flask scraped to release the cells from the floor of the flask. The cells were then re-suspended and pipetted into new flasks (4 mL for T-25, 15 mL for T-75).

To freeze SHSY cells, confluent T-75 flasks were scraped and the cell suspension centrifuged for five minutes at 6500 rpm. The supernatant was aspirated, and 1 mL of pre-warmed freezing medium (Gibco) was added. The cells were re-suspended, pipetted into a

freezing vial, and stored at -80°C in a Styrofoam® rack for insulation to slow the freezing process. After 24 hours, the cells were moved to liquid nitrogen storage.

For plating experiments, 70 to 75% confluent T-75s were aspirated, trypsinized for approximately two minutes at 37°C with 5 mL of 0.25% Trypsin-EDTA (Gibco), then re-suspended with 10 mL pre-warmed medium in a 15 mL conical tube. The cell suspension was centrifuged, aspirated, and the cell pellet was re-suspended in 24 mL of pre-warmed medium and plated into six T-25s, each containing a total of 4 mL cell suspension. For Aβ treatment conditions, Yankner peptide (Tocris; see below) was introduced to flasks at 20 µM (80 µL of 1 mM stock per 4 ml medium). For hEPN treatment conditions, hEPN-1 peptide (BioTherapeutix, Inc.) was introduced to flasks at 150 µM (160 µL of 3.75 mM stock per 4 ml medium). Untreated, control flasks generally reached approximately 80% confluency after 72 hours, at which point cells were subjected to morphology and trypan blue exclusion cell counts (see below) and harvested by scraping to prepare whole cell lysates.

Yankner Peptide

Human Yankner peptide ($A\beta_{25-35}$) was purchased from Tocris Bioscience (#1429, Batch 5B). The peptide was stored in 1 mM stock suspension (1 mg, 943 nmol peptide added to 0.94 mL of 1 mM sodium bicarbonate) at -20°C. The Yankner peptide was used at a final concentration of 20 µM in human SHSY cell culture, which has been proven sufficient previously in our lab for producing neurotoxic effects.

hEPN-1 Neurotrophic Factor

Several human ependymin–1 (hEPN-1) peptides containing the same amino acid sequence in different salt conditions were provided by BioTherapeutix, Inc. (Brookline, MA) or CS Bio Company (Menlo Park, CA). Peptides were received as dry powders and stored at

-20°C. For plating experiments, hEPN-1 peptides were used at a final concentration of 150 µM (1 mg of peptide added to 1 mL of filtered DMEM-F-12 medium).

Cell Morphology Counts

Three representative regions of each experimental flask were imaged at 72 hours post-plating by a Leica inverted microscope and camera attachment at 20x magnification. Images were used to count cells with free stellate morphologies, physically networked morphologies, and free non-stellate (lacking protrusions, or "balled up") morphologies, as well as total cells per viewing field. Counts from all three representative regions of flasks were averaged to provide final morphology estimates as a percentage of total cell counts.

Trypan Blue Exclusion Viability Assay

Cell suspensions harvested from experimental flasks were vortexed, and 10 µL aliquots of suspension were transferred to a 1.5 mL eppendorf tube. Each aliquot was vortexed and pipetted onto a clean microscope slide with an equal volume of 0.4% Trypan Blue (Gibco), and the solution was mixed using a pipette tip and spread to create an area of about 1cm by 1cm. Three representative regions of each slide were imaged (as described above), and images were used to count total viable (Trypan Blue-excluding) and non-viable cells. Counts from all three representative images were again averaged to provide final viability estimates as a percentage of total cell counts.

SHSY Whole Cell Lysates

Experimental T-25 flasks were harvested via scraping, and the cell suspensions were transferred to 15 mL conical tubes and centrifuged for five minutes at 500x g to obtain cell pellets, disregarding pre-selection for lysosomes. After reserving 1 mL of supernatant for

assaying, the remaining supernatant was aspirated and 200 µL of Complete Lysis Buffer [20 mM HEPES pH 7.9, 10 mM KCl, 300 mM NaCl, 1 mM $MgCl_2$, 0.1% Nonidet P40, 20% glycerol, 0.5 mM DTT (Gibco; added fresh) and 0.5 mM PMSF (Sigma; added fresh)] was added to each pellet, and the re-suspended pellet transferred to a 1.5 mL microfuge tube. Suspensions were incubated on ice for five minutes with occasional vortexing to ensure lysis, after which lysates were microfuged for five minutes at 13,000 rpm to pellet cell debris. The clarified supernatant was aliquoted into eppendorf tubes, and stored at -80°C.

Cathepsin-D Activity Assays

All Cat-D activity assays were performed using a Cathepsin-D Activity Assay Kit (Sigma, CS0800) designed to quantify Cat-D activity in solution by measuring the fluorescence of MCA (7-methoxycoumarin-4-acetyl) released from the substrate (MCA-Gly-Lys-Pro-Ile-Leu-Phe-Phe-Arg-Leu-Lys(DNP)-D-Arg-NH_2) in response to enzyme-substrate binding. The manufacturer's protocol, which described the kit's application to 100 µL reactions prepared in 96-well plates and assessed by plate readers, was adapted for use with a single 100 µL microcuvette via the preparation of reactions in microfuge tubes, individual processing of reactions, and intermittent cuvette cleaning with 0.1 N Nitric Acid followed by distilled water. An MCA standard curve was established from MCA Standard Solution (Sigma) to relate MCA concentration to fluorescence, and to optimize fluorimeter settings to the protocol. The medium and lysate preferences were established for the assay protocol, and Pepstatin A- inhibited reactions were used to demonstrate near complete enzyme-substrate specificity and the effectiveness of three minute time courses (see Results).

For assay preparation, SHSY cell lysates were thawed from -80ºC storage, and added to 100 µL total volume Cat-D activity assay reactions, prepared in 0.5 mL microfuge tubes and adjusted for a 1:5 lysate-to-reaction volume ratio from the manufacturer's suggested

protocol. Immediately upon the addition of Cat-D substrate (Sigma), the tube was flicked briefly to mix, and the fluorescence was quantified by fluorimeter (Photon Technology International) and PTI software through single point captures at 20 second intervals over three minutes with default settings and excitation wavelength 328 nm, emission wavelength 389 nm, excitation (Ex2) slit width 1.25 nm or 0.31 mm (W), and gated detectors at 50% emission. For treatment comparisons, fluorescence values were adjusted for baseline by subtracting values from a blank reaction (without enzyme) at each time point. Purified Cat-D (0.1 unit/mL purified bovine spleen Cat-D, Sigma) was also run at a 1:5 enzyme-to-reaction volume ratio as a positive control.

RESULTS

Genotyping of Transgenic Alzheimer's Mice

Our laboratory's Alzheimer's mouse colony is maintained long-term by breeding normal non-transgenic (WT) females to 5X transgenic males (AD mice). Because the offspring can either be WT or transgenic, and the genotype is not obvious by coat color, genotyping was performed post-mortem on brain tissue. To help ensure a more accurate assessment, both human APP and PSEN transgenes were measured in both crude alkaline tissue lysates and purified DNA.

Genotyping was initiated in our lab over the summer, and was then completed in this project with a particular focus on mice which proved difficult to genotype. PCR samples were separated by electrophoresis through 2.5% agarose gels, and gels were photographed by UV trans-illumination (**Figure-7A**). Gels from the PCR reactions of two independent alkaline lysates and six phenol extractions were considered in determining consensus genotypes for five previously unknown mice (**Figure-7B**). Two known negative and known positive transgenic mice were used as experimental controls.

A

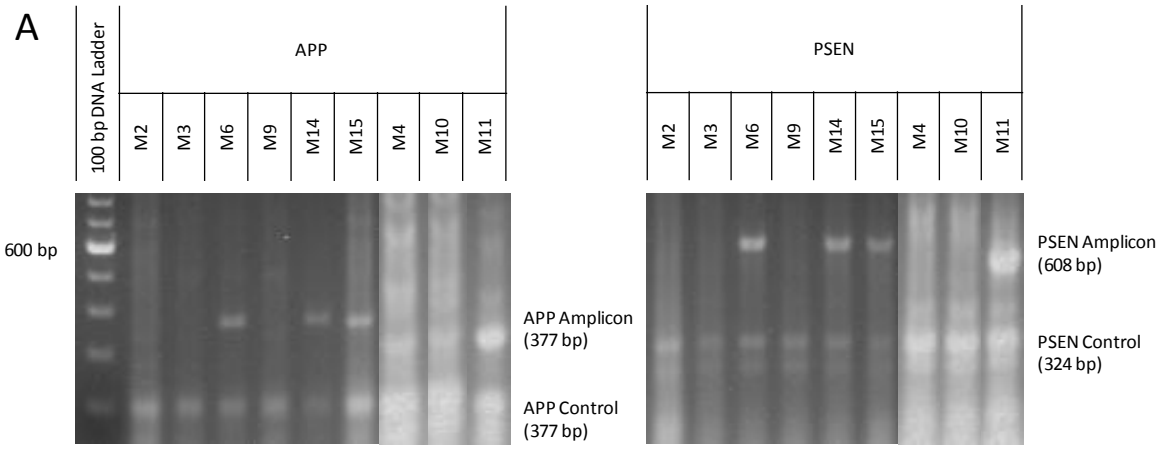

B

Alkaline Lysis		Known (+)		Known (-)		Unknown				
		M3 (N=2)	M6	M2	M10	M4 (N=2)	M9 (N=2)	M11 (N=2)	M14 (N=2)	M15 (N=2)
	APP	-				-	-	+	+	+
	PSEN	-				-	-	+	+	+

DNA Purification		Known (+)		Known (-)		Unknown				
		M3 (N=4)	M6 (N=2)	M2 (N=6)	M10 (N=2)	M4 (N=6)	M9 (N=6)	M11 (N=2)	M14 (N=4)	M15 (N=5)
	APP	+	+	-	-	-	-	+	+	+
	PSEN	+	+	-	-	-	-	+	+	+

Figure-7: Confirmation of Transgenic Alzheimer's Mouse Genotypes. DNA from unknown mice (arbitrary identifiers M4, M9, M11, M14, M15) was isolated from brain tissue by both alkaline lysis and phenol extraction techniques, then amplified by PCR for human APP and PSEN transgenes. Amplified DNA was separated by electrophoresis through 2.5% agarose gels then photographed by UV trans-illumination. **A**. Representative gel lanes from brain phenol extracted DNA of two known positives (M3, M6), two known negatives (M2, M10), and five unknown mice. The lower band in each reaction represents a load control amplified from a non-transgenic gene. **B**. Summary table of consensus genotypes for five unknown mice (arbitrary identifiers M4, M9, M11, M14, and M15) determined from two alkaline lysates and six phenol extractions. Known positives (M3, M6) and negatives (M2, M10) were included as experimental controls.

SOD

Immunoblots were used to determine the cellular levels of superoxide dismutase (SOD-1) in the brains of nine month old AD mice treated with vehicle (N=8) or 2 mg/kg

hEPN (N=8) by oral gavage. Whole cell lysates of harvested brain tissue, thawed from -80ºC storage, were separated by PAGE, electroblotted to nitrocellulose membrane, then probed for both SOD-1 (16 kDa) and housekeeper tubulin (55 kDa) (**Figure-8A**). The mean optical density of each band was analyzed by Scion image analysis software, which demonstrated a statistically significant increase (student's t-test, $p<0.01$) in SOD-1 for the hEPN-treated mice (**Figure-8B**). These results indicate that the cellular levels of anti-oxidative SOD-1 were significantly elevated in hEPN treated AD mice relative to vehicle treated controls.

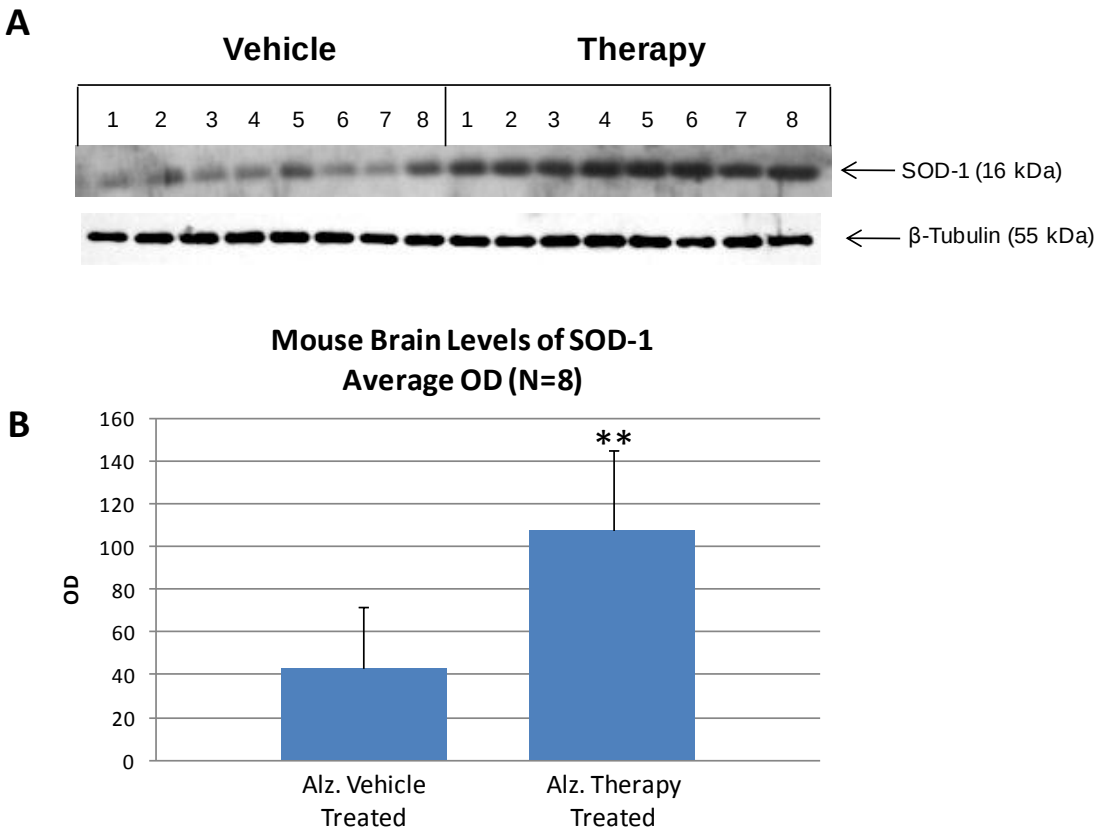

Figure-8: Brain SOD-1 Levels Increase with hEPN *in vivo*.
Proteins in brain lysates from eight vehicle-treated AD transgenic mice and eight hEPN-1-treated AD mice were separated by PAGE, blotted to nitrocellulose, and probed for SOD-1 and load control tubulin. All blots were run simultaneously with SOD-1 using a 2µg total protein load and β-Tubulin using a 5µg total protein load. **A.** Immunoblot results (N=8) for SOD-1 (16 kDa) and β-tubulin (55 kDa). Protein was detected by SuperSignal West Pico chemiluminescent substrate (Pierce), and exposed to Biomax XAR-5 film (Kodak) for four minutes (tubulin) or one second (SOD). Film was developed automatically in the Kodak M35A X-Omat Processor. **B.** Analysis of the optical density (OD) of the immunoblot image in panel A by Scion software. Brain SOD-1 levels significantly increase ($p<0.01$) in AD mice following treatment for two weeks with 2 mg/kg hEPN by oral gavage. Error bars indicate one standard deviation.

In vitro Alzheimer's Model with Aβ and hEPN

Our laboratory previously showed that treating cultured human SHSY neuronal cells with Aβ acts as an *in vitro* model for AD. The Aβ treatment was shown to decrease cell survival (Stovall, 2006), increase caspase-3 (Kapoor, 2007), increase tau hyper-phosphorylation, and increase TUNEL staining (Ronayne, 2008). Further, treating the cells simultaneously with Aβ and goldfish EPN decreased those events. This project extended these previous studies by investigating human, rather than goldfish, EPN treatments, and by analyzing the theorized mediator of cell death cathepsin-D.

Trypan Blue Exclusion Viability Counts

Trypan Blue staining was used to investigate cell viability in our *in vitro* AD model. Viable cells exclude Trypan Blue stain because the dye cannot pass through the intact cell membrane, resulting in the white "halo" observed around these healthy cells. Alternately, non-viable cells absorb Trypan Blue stain because the dye can leak through the depolarized cell membrane, resulting in the very dark blue color exhibited by these damaged cells.

As in our lab's previous projects, the shorter Yankner peptide was used as a substitute for Aβ due to its increased solubility while still retaining the receptor binding domain necessary for the induction of cell death. SHSY cells treated with Yankner peptide or Yankner plus hEPN at 24 hours, or left untreated as a negative control, were harvested at 72 hours post-plating and stained with Trypan Blue (Gibco; **Figure-9A**). The Yankner treated cultures showed an observable increase in the percentage of non-viable cells relative to untreated control cultures, and a slight reversal of this viable–to-non-viable cell ratio occurred in Yankner plus hEPN treated cells. The percent of viable and non-viable cells were calculated for two independent plating experiments, using three representative images from

each treatment. The data show a statistically significant decrease (student's t-test, $p<0.01$) in viable cells from Yankner treated cultures relative to untreated cultures. The data also indicated a slight recovery in viable cells for the Yankner plus hEPN culture relative to the Yankner culture (**Figure-9B**).

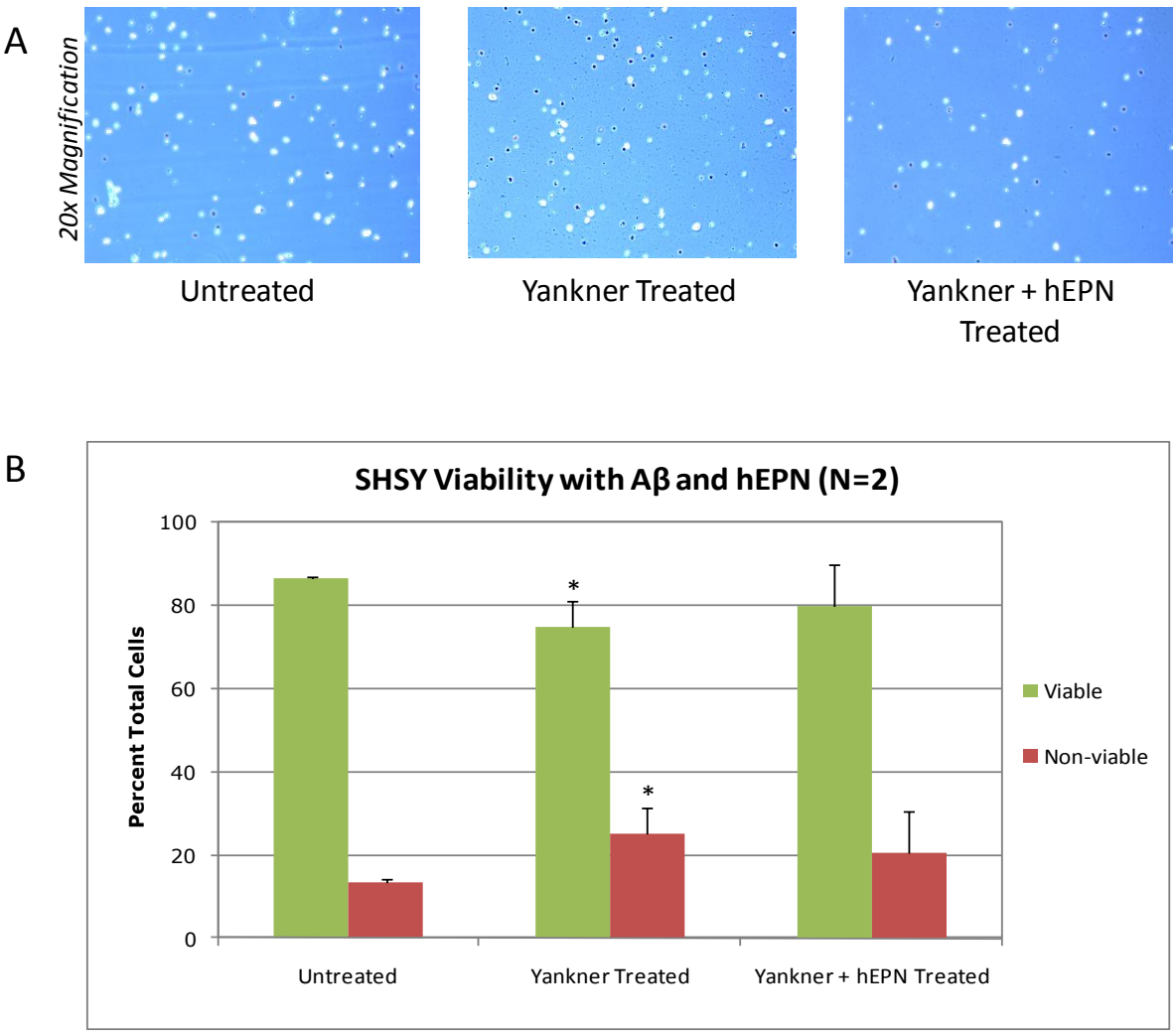

Figure-9: Analysis of Cell Viability.
Human SHSY neuroblastoma cells were treated with Yankner, Yankner plus hEPN, or left untreated at 24 hours post-plating. **A.** Shown are three representative photomicrographs at 20x magnification after cells were harvested and stained with Trypan Blue at 72 hours post plating. An increase in the percentage of blue non-viable cells demonstrated that Yankner is neurotoxic at 20 μM (center panel), while hEPN at 150 μM (right panel) partially rescues the percentage of viable cells back to untreated levels. **B.** Averaged data from two independent viability assays demonstrated a decreased ratio of viable-to-non-viable cells in Yankner treated culture relative to untreated culture ($p<0.01$), and a partial rescue with hEPN treatment. Error bars indicate one standard deviation.

Cell Morphology Counts

Cell morphology was also investigated in our *in vitro* AD model as another measure of Yankner-induced neurotoxicity and potential hEPN rescue. Three representative regions of various cultures were imaged by a Leica inverted microscope and camera attachment (**Figure-10A**). In these cultures, normal, healthy SHSY cells maintained a stellate morphology and numerous intercellular connections, while damaged SHSY cells displayed an abnormal rounded morphology with few connections. Morphology counts for free stellate, physically networked, and free non-stellate morphologies were calculated as percentages of total cell counts, and averaged over three independent plating experiments. The data showed a statistical increase in free non-stellate morphology and a statistical decrease in physically networked morphology within Yankner treated cultures relative to untreated control ($p<0.001$; **Figure-10B**), as well as a nearly complete rescue by hEPN.

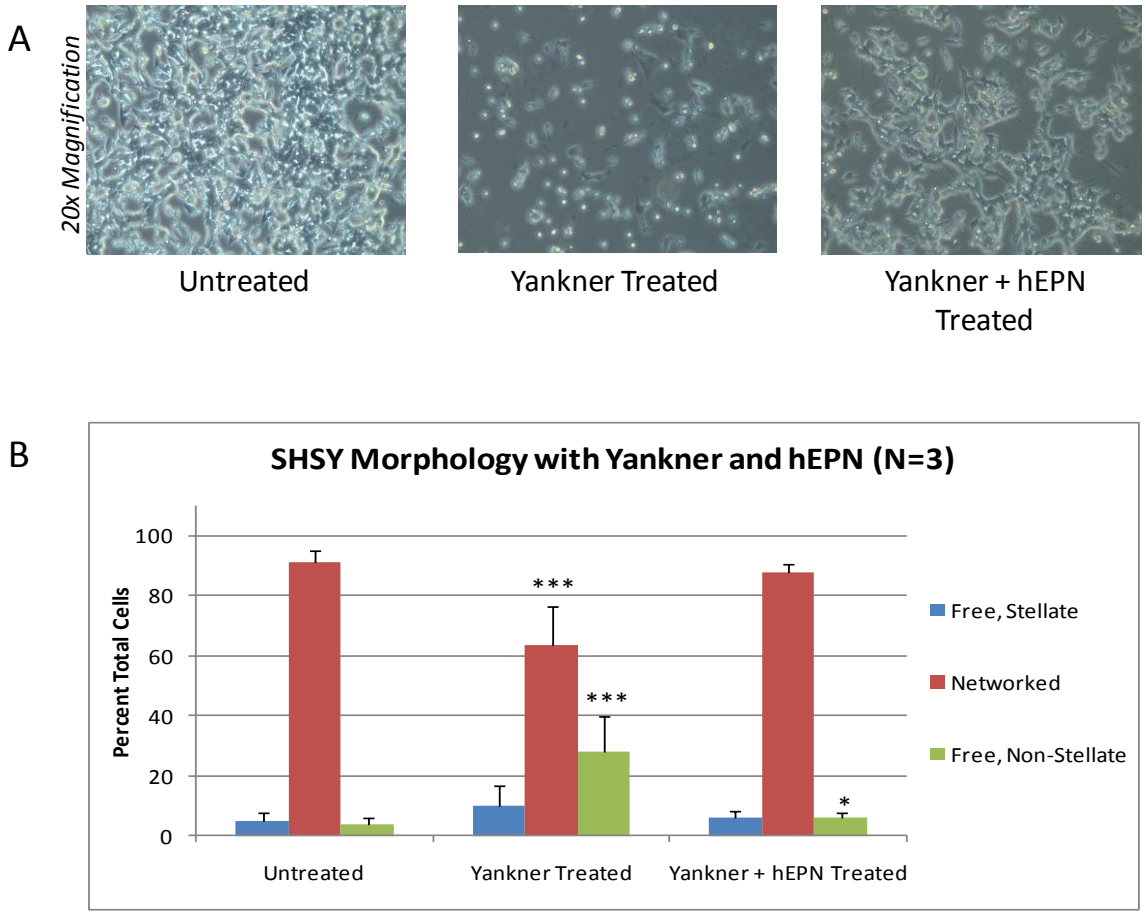

Figure-10: Analysis of Cell Morphology in Response to Yankner and hEPN. Human SHSY neuroblastoma cells were treated with Yankner, Yankner plus hEPN, or left untreated at 24 hours post-plating. **A**. Representative images of Yankner treated, Yankner plus hEPN, and untreated SHSY cultures, taken at 72 hours post-plating by a Leica inverted microscope and camera attachment with 20x magnification. The data illustrate neurotoxicity of Yankner peptide at 20 µM, and significant rescue by hEPN at 150 µM. **B**. Quantitation of cell morphology counts confirm that Yankner toxin significantly decreases the percentage of networked cells while increasing non-stellate morphology relative to untreated control ($p<0.001$), with a near complete rescue by hEPN ($p<0.05$).

Cathepsin-D Fluorescent Substrate Activity Assays

According to a litany of recent research, the lysosomal aspartic protease cathepsin-D (Cat-D) correlates with a variety of both pathogenic and therapeutic intracellular pathways. In some cases, studies showed Cat-D involvement in apoptotic pathways leading to caspase initiation and cell death, while other research Cat-D has been associated with the degradation and clearance of toxic aggregations such as those characteristic of Alzheimer's disease. Due to this largely unresolved debate, and the lack of research to our knowledge regarding Cat-D

enzymatic activity in Aβ cascade models, the second primary goal of this project was to establish a successful Cat-D activity assay protocol for our SHSY *in vitro* Alzheimer's model, and to use this assay to observe the effects of our established Yankner insult and hEPN rescue on Cat-D activity.

A Cathepsin-D Activity Assay kit (Sigma, CS0800) designed for 100 µL reaction volumes was used to quantify Cat-D activity in solutions by measuring the fluorescence of MCA (7-methoxycoumarin-4-acetyl) released from the substrate (MCA-Gly-Lys-Pro-Ile-Leu-Phe-Phe-Arg-Leu-Lys(DNP)-D-Arg-NH_2) in response to enzyme-substrate binding. The manufacturer's protocol was adapted for use with a single 100 µL microcuvette via the preparation of reactions in microfuge tubes, individual processing of reactions, and intermittent cuvette cleaning with 0.1 M Nitric Acid and distilled water.

An MCA standard curve, relating MCA fluorescence to known concentrations in solution, was first established ($R^2 = 0.9814$) for the adjusted fluorimeter and microcuvette system over an MCA concentration gradient of 0.25 to 1.5 nmoles (**Figure-11**). The fluorimeter excitation and emission wavelengths (328 nm, 389 nm) were also optimized for MCA fluorescence based on these variable concentration trials (data not shown).

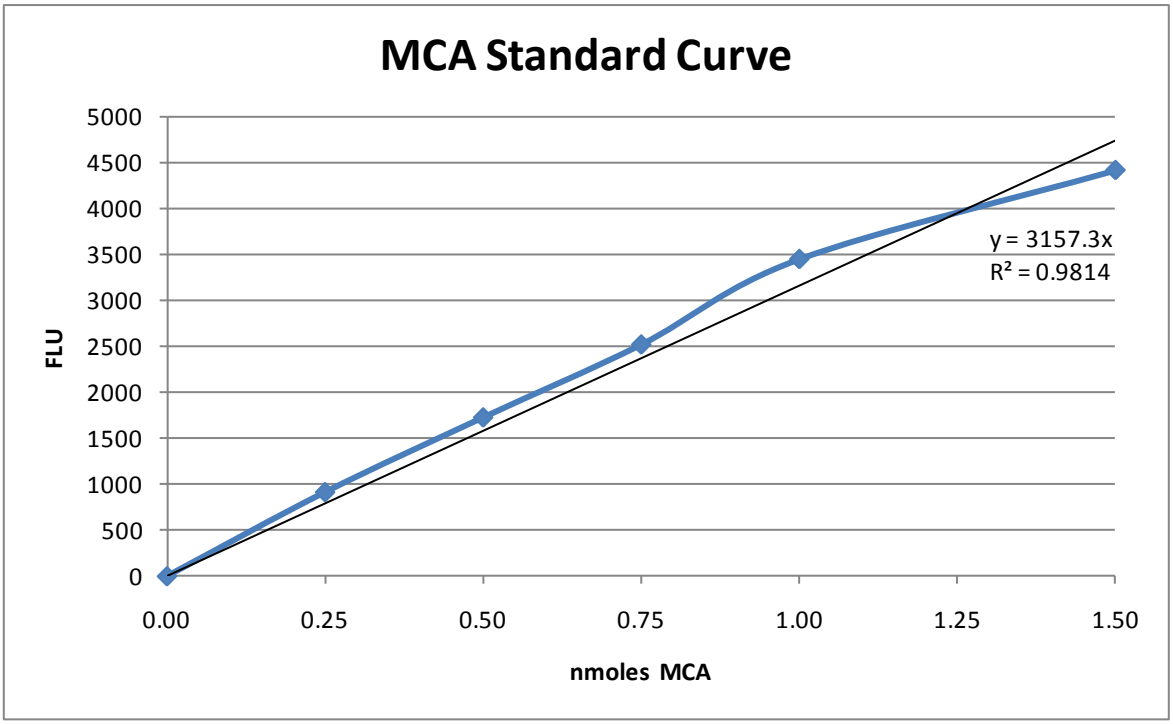

Figure-11: Fluorescent MCA Standard Curve for Cat-D Activity Assay.
MCA (7-methoxycoumarin-4-acetyl) standard solution (Sigma) was diluted with assay buffer (Sigma) to concentrations 0.25, 0.50, 0.75, 1.00, 1.25, and 1.50 nmoles in 100 µL total volumes, and fluorescence was measured individually. Fluorescence values were plotted against MCA concentration, and linearly regressed with origin 0.00 to provide a slope of 3157.3 with $R^2 = 0.9814$.

In order to adapt the activity assay to SHSY lysates, the viability of Cat-D in the presence of culture medium and SHSY lysis buffer was established. Undiluted culture medium and whole cell lysates (20 µL) were added to 100 µL total volume reactions and allowed to incubate immediately upon the introduction of substrate for 30 minutes at 37ºC. At 30 minutes, MCA fluorescence was quantified by fluorimeter (**Figure-12A**), indicating that Cat-D was barely active within culture medium but significantly active in cultured cells. To assure that the culture medium was not interfering with fluorescence data, 0.001 units (10 µL) of 0.1 unit/mL purified Cat-D from bovine spleen (Sigma) was introduced to either 10 µL medium or 10 µL lysate reactions, and fluorescence was measured after a 30 minute incubation at 37ºC (**Figure-12B**). This data demonstrated insignificant inhibition of exogenously added Cat-D enzyme by the culture medium relative to pure Cat-D alone (blue

and green histobars, panel B). Thus, while the culture medium did not interfere with the activity assay, it was not found to be a significant source of Cat-D activity.

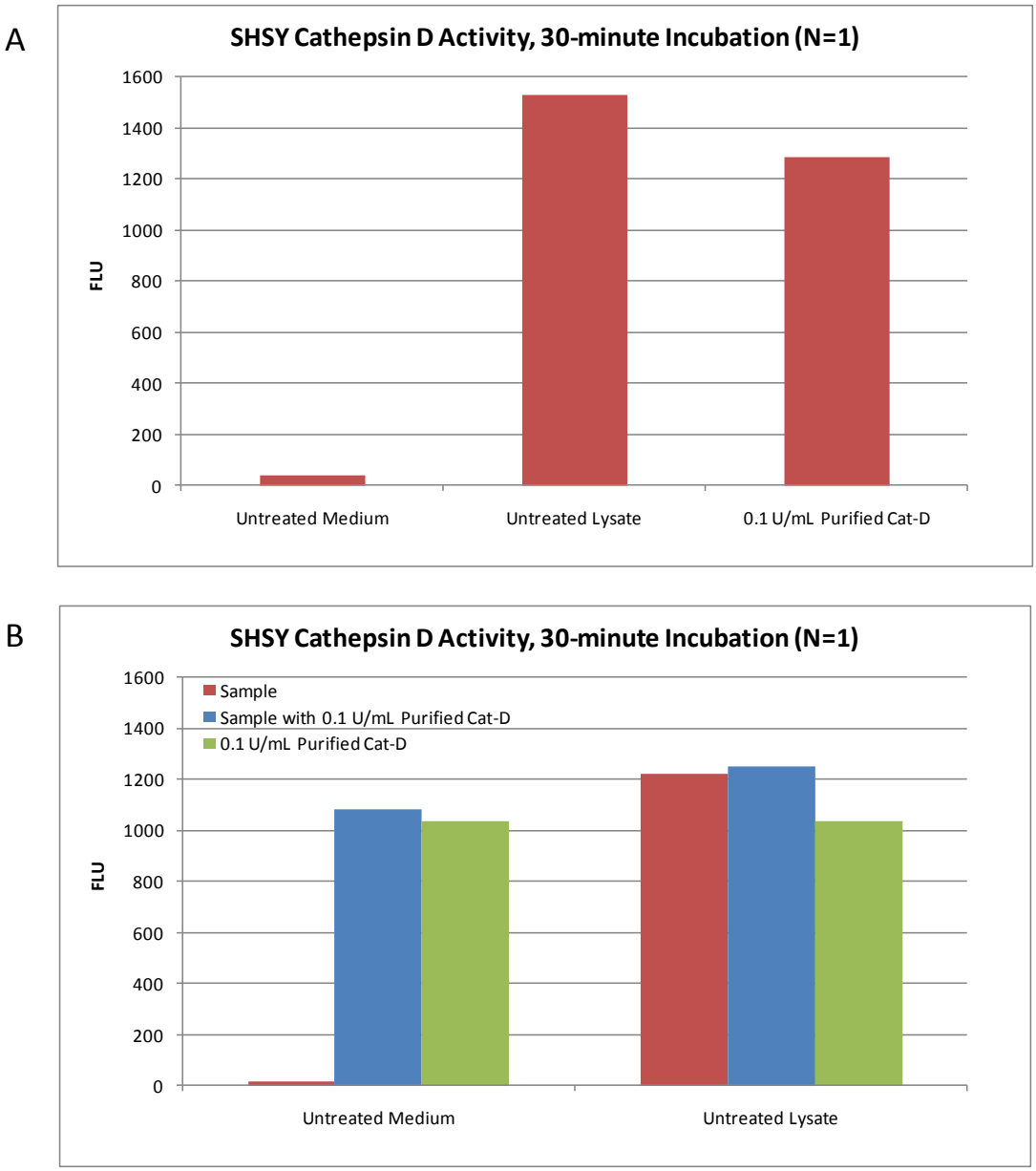

Figure-12: Establishment of Cell Lysis Buffer as Preferable over Culture Medium for Cat-D Activity Assays.
Undiluted medium or whole cell lysate from an untreated SHSY culture, together with 0.1 unit/mL purified bovine spleen Cat-D positive control (20 µL total), were added to 100 µL total reaction volumes and incubated for 30 minutes at 37ºC to determine viability and relative Cat-D activity of each. **A**. Fluorescence from representative assay of culture medium, lysates, and 0.1 U/mL purified Cat-D, corrected for baseline (blank), demonstrated a lack of Cat-D activity in culture medium, with most of the activity instead residing within the cell lysate. **B**. Fluorescence from representative assay of culture medium and lysates with and without 0.1 U/mL purified Cat-D, corrected for baseline (blank), validated viability of both medium and lysates for activity assay.

To establish the specificity of the substrate for Cat-D present in whole cell lysates and purified from bovine spleen (Sigma), and to establish the potential for performing activity time-courses, three minute activity assays (N=3) were performed on uninhibited and Pepstatin-A-inhibited reactions. The fluorescence was recorded at 20 second intervals (**Figure-13A**), averaged, and adjusted for baseline (blank) (**Figure-13B**). The data showed fluorescence values within an acceptable range (0-4000 FLU), leading to the adoption of three minute time-courses in all subsequent assays without need for the sensitivity of the 30 minute reactions. The data also showed that Pepstatin-A-inhibited reactions exhibited low fluorescence even below baseline values, indicating that Cat-D, rather than other proteases present in culture lysates, was solely responsible for substrate cleavage. Thus, the fluorescence recorded in subsequent assays was attributed to Cat-D activity alone.

A

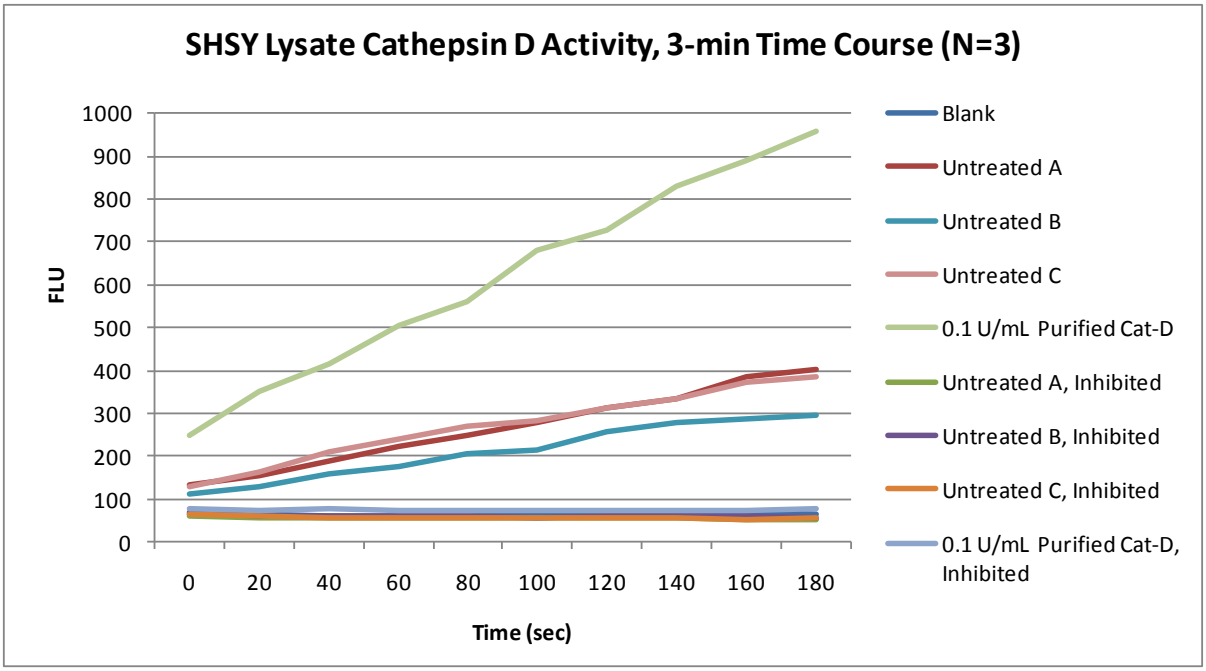

B

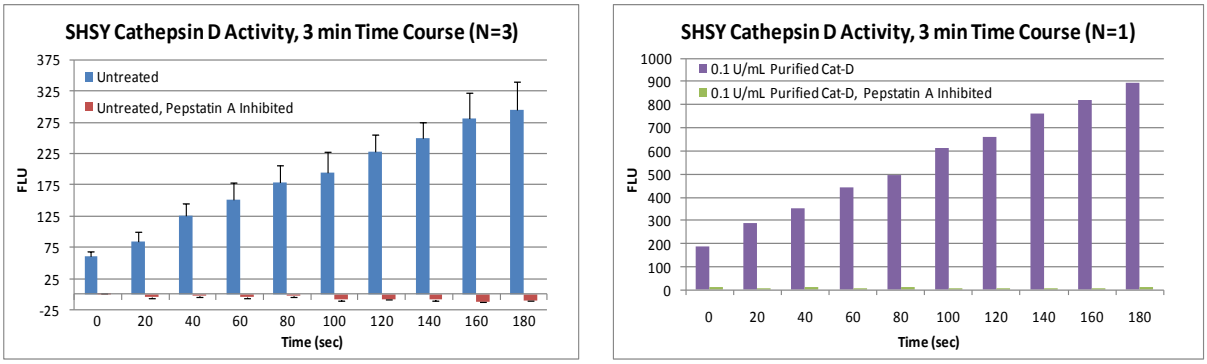

Figure-13: Cat-D Substrate Specificity.
Undiluted whole cell lysate from untreated SHSY cultures (N=3) and purified bovine spleen Cat-D positive control (20 µL each) were added to 100 µL total reaction volumes and fluorescence was recorded by fluorimeter immediately upon introduction of substrate at 20 second intervals for three minutes to determine specificity of Cat-D and substrate. **A**. Fluorescence from uninhibited lysate reactions was within acceptable range (0-4000 FLU) and distinct from that of blank and 0.1 U/mL purified Cat-D, while fluorescence from inhibited lysate reactions was equal or below baseline. **B**. Average fluorescence from three uninhibited and inhibited lysate reactions (left) and one uninhibited and inhibited 0.1 U/mL purified Cat-D reaction (right), corrected for baseline (blank) fluorescence. Insignificant fluorescence of corrected inhibited reactions demonstrated near complete specificity of the substrate for Cat-D enzyme.

After establishing the main Cat-D reaction format, and demonstrating its effectiveness for measuring Cat-D activity alone, the assay was then applied to Yankner treated cultures. The assay was used to monitor the effect of Yankner treatment at time of plating and 12, 24, 36, and 48 hours post-plating. The fluorescence of undiluted reactions from SHSY cultures

treated at 24-hour intervals (**Figure-14A**) and 12-hour intervals (**Figure-14B**) was recorded by fluorimeter and adjusted for baseline (blank). Yankner treatment at 24 hours post-plating produced optimal Cat-D activity over all alternate conditions, establishing this condition as the standard treatment schedule for all subsequent experiments.

A

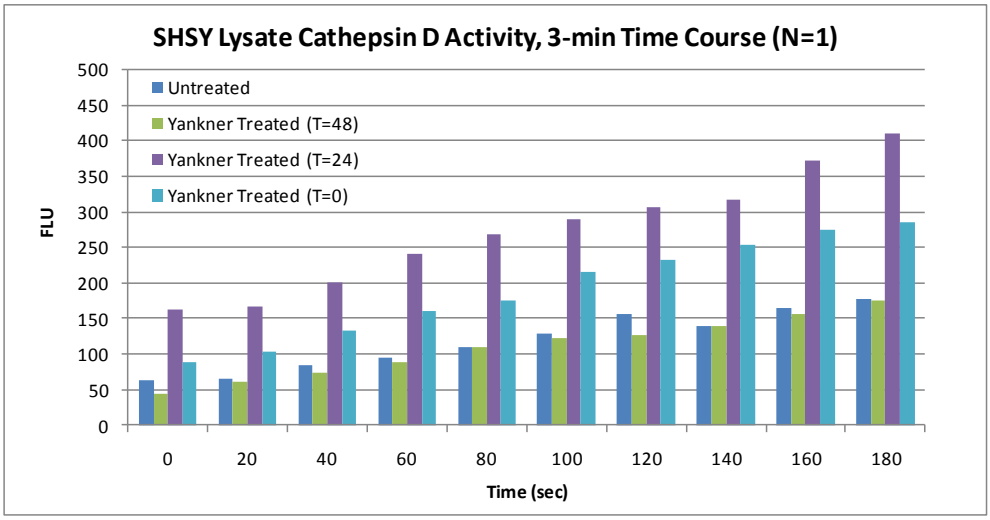

B

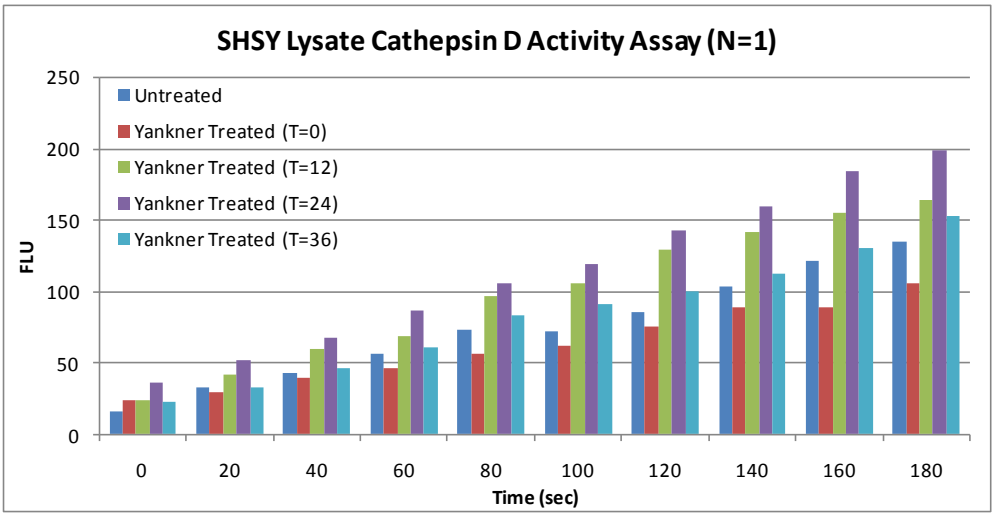

Figure-14: Cat-D Activity in SHSY Cells Following Yankner Treatment. Undiluted whole cell lysates from SHSY cultures treated with Yankner peptide at 24-hour and 12-hour intervals post-plating (20 µL each) was added to 100 µL total reaction volumes and fluorescence was recorded by fluorimeter immediately upon introduction of substrate at 20 second intervals for three minutes to determine optimal Yankner regimen for inducing Cat-D activity. Blank and 0.1 U/mL purified Cat-D reactions (not shown) validated each assay. **A**. Representative assay of lysates from Yankner treated cultures at 0, 24, and 48 hours post-plating, adjusted for baseline (blank). The Yankner treatment at 24 hours post-plating (purple histobars) demonstrated the highest Cat-D activity. **B**. Representative assay of lysates from Yankner treated cultures at 0, 12, 24, 36, and 48 hours post-plating, adjusted for baseline (blank). Again, Yankner treatment at 24 hours post-plating (purple histobars) demonstrated highest Cat-D activity.

Using this optimized 24 hr post-plating Yankner addition for the SHSY *in vitro* AD model, the assay was repeated (N=3) to assess significance and repeatability (**Figure-15**). In all cases, Yankner treatment at 24 hours post-plating produced significantly elevated Cat-D activity in SHSY lysates relative to lysates from untreated cultures.

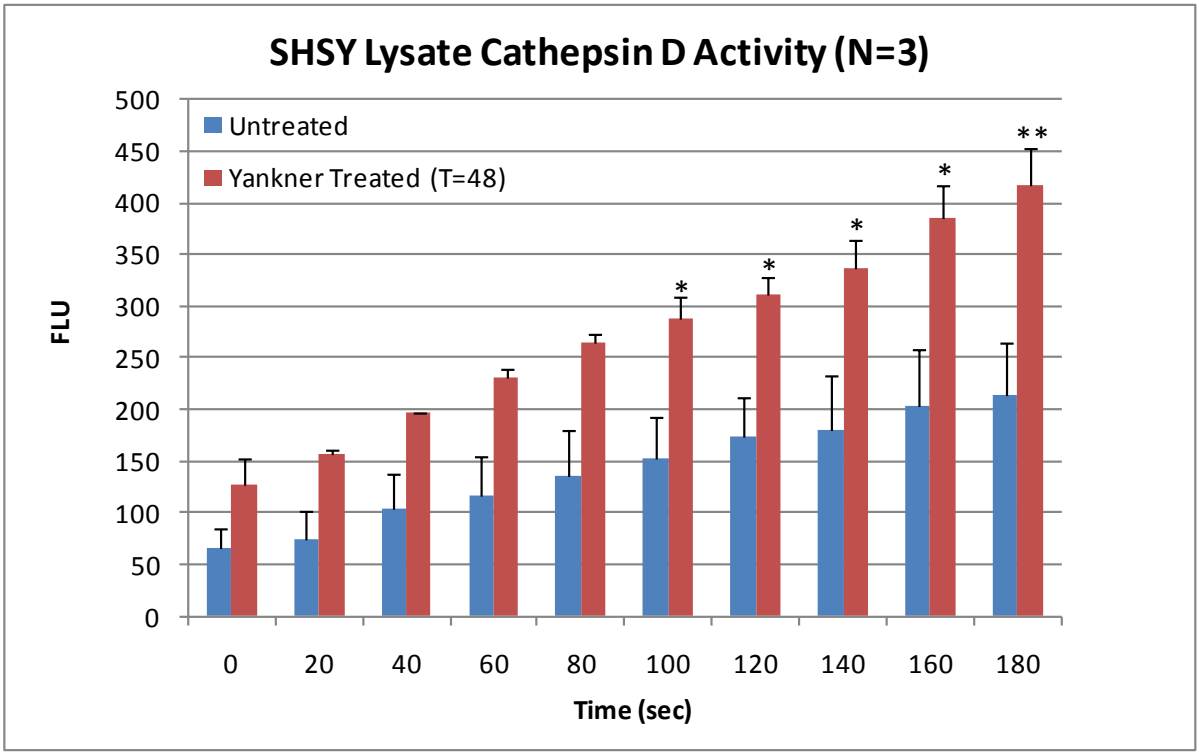

Figure-15: Cat-D Activity in Yankner Treated SHSY Cells Relative to Untreated Controls.
Undiluted whole cell lysates from SHSY cultures treated with 20 µM Yankner peptide at 24-hours post-plating or left untreated (20 µL each) were added to 100 µL total reaction volumes and fluorescence was recorded by fluorimeter immediately upon introduction of substrate at 20 second intervals for three minutes. Blank and 0.1 U/mL purified Cat-D reactions (not shown) validated each assay. Fluorescence from lysates of Yankner treated cultures (N=3) demonstrated observably increased fluorescence over lysates of untreated cultures (N=3; all fluorescence values adjusted for baseline), with statistical significance at time points 100, 120, 140, 160, and 180 seconds (student's t-test; * = $p<0.05$, ** = $p<0.01$). Error bars denote one standard deviation.

In order to determine whether treatment of SHSY cells with hEPN could lower the Yankner-induced increase in Cat-D activity, the assay was applied to untreated, Yankner treated, and Yankner plus hEPN-treated cultures (**Figure-16**). In the single preliminary trial of this experiment, EPN treatment appeared to produce the highest Cat-D activity at all time points tested.

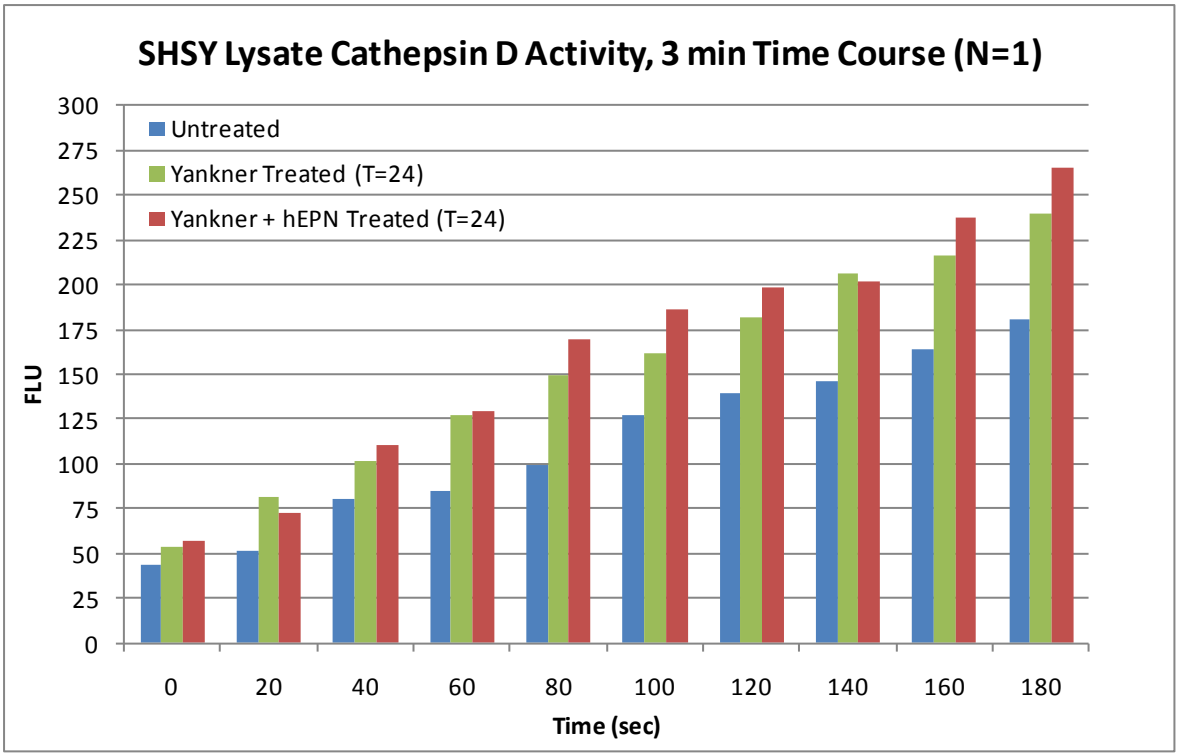

Figure-16: Cat-D Activity in SHSY Cells Following Yankner and Yankner plus hEPN Treatment.

Undiluted whole cell lysates from SHSY cultures treated with 20 µM Yankner peptide, 20 µM Yankner peptide plus 150 µM hEPN, or untreaed at 24-hours post-plating (20 µL each) were added to 100 µL total reaction volumes and fluorescence was recorded by fluorimeter immediately upon introduction of substrate at 20 second intervals for three minutes. Blank and 0.1 U/mL purified Cat-D reactions (not shown) validated the assay. Preliminary assay of all three conditions, adjusted for baseline (blank), demonstrated increased fluorescence in Yankner treated culture lysates relative to untreated culture lysates, and further increased fluorescence in Yankner plus hEPN treated culture lysates relative to lysates of both untreated and Yankner treated conditions.

DISCUSSION

This project was undertaken to extend our laboratory's previous studies of both *in vitro* and *in vivo* systems for mimicking Alzheimer's disease. It has been shown by our lab that treating cultured human SHSY neuronal cells in the presence of Yankner peptide decreases cell viability (Stovall, 2006), activates caspase-3 (Kapoor, 2007), and increases tau hyper-phosphorylation and TUNEL staining (Ronayne, 2008). Treatment with goldfish EPN partially reversed these effects, while also increasing cellular inhibitors of apoptosis (cIAPs) (Rawal, 2009). This project further extended these studies through the analysis of human EPN in a similar *in vitro* model with a focus on the theorized mediator of cell death, cathepsin-D. Past studies in our lab which analyzed the effects of human EPN on transgenic Alzheimer's mice *in vivo* were also extended in this project with particular focus on the anti-oxidative enzyme superoxide dismutase 1 (SOD-1).

SOD

As AD cell death is known to involve increases in reactive oxidative stress (ROS), we hypothesized that treatment with a NTF might increase cellular levels of enzymes known to reduce ROS, such as superoxide dismutase 1 (SOD-1). In the brains of nine-month old transgenic Alzheimer's mice treated with hEPN neurotrophic factor for two weeks, cellular levels of therapeutic anti-oxidative SOD-1 assayed by immunoblots (N=8) were significantly ($p<0.01$) increased relative to vehicle-treated mice. This indicates that AD mice treated with hEPN are able to increase SOD-1 production *in vivo*. Therefore, hEPN-treated mice should be better able to catalyze the dismutation of anionic superoxide, resulting in the reduction of oxidative stress and apoptosis in brain cells – a conclusion which may also help to explain our earlier results indicating that Yankner plus hEPN treatment of SHSY cells increases cell

survival over Yankner treatment alone. This line of experimentation could be extended in future studies by assaying other enzymes known to alleviate ROS, including catalase and glutathione peroxidase.

In vitro Alzheimer's Model with Aβ and hEPN

Normal SHSY neuronal cells have a stellate morphology and form numerous inter-cellular connections. In our *in vitro* tests with cultured SHSY cells, Yankner neurotoxin (mimicking Aβ) was found to significantly decrease the percentage of connected neuronal cells ($p<0.001$) and increase cells with non-stellate morphology ($p<0.001$), while hEPN treatment demonstrated a near complete rescue of these effects ($p<0.05$). A trypan blue viability assay similarly demonstrated significant loss of cell viability with Yankner treatment ($p<0.01$) and slight rescue by hEPN. While the establishment of the *in vitro* system was time consuming, requiring the testing of various batches of Yankner for solubility and potency, these findings prove that Yankner is neurotoxic and reduces the number of networked, viable cells *in vitro,* validating our *in vitro* AD model and in turn supporting the amyloid cascade hypothesis (see Background) which proposed that Aβ formation initiates AD *in vivo*. This data also illustrated the capability of *human* hEPN therapeutic treatment to partially rescue Aβ-induced apoptosis.

Cathepsin-D Activity Fluorescent Substrate Assays

The major portion of this project was spent developing a fluorescent substrate assay for cathepsin-D (Cat-D) activity. Following the treatment of cultured human SHSY neuroblastoma cells *in vitro* with Yankner peptide, Cat-D enzyme activity was shown to significantly increase ($p<0.05$ or $p<0.01$) relative to untreated cultures. Further, treatment of identical samples with Pepstatin-A inhibitor confirmed that the increased fluorescence

observed in Yankner treated lysates could be attributed solely to enzymatic Cat-D activity, rather than other unrelated proteases. These results suggest that Yankner treatment elevates Cat-D activity in SHSY culture, hinting that Cat-D may play a role in the cellular responses to this toxin *in vitro* and, potentially, within the *in vivo* AD mouse model. The reason for this increased Cat-D activity is not yet clear, however, and previous research supports roles in both the therapeutic degradation of apoptotic proteins and the damaging mediation of cell death. This dilemma could be directly addressed in future studies using RNAi to knockdown Cat-D expression in SHSY cells prior to Yankner treatment, elucidating whether the presence of Cat-D is required for Yankner induced cell death. Yet regardless of the outcomes, our data suggest that Aβ likely plays a role in the cellular apoptotic pathways of AD.

Future Recommendations

At this time, we were unable to clearly demonstrate whether hEPN treatment lowers or increases Cat-D levels *in vitro*. Further plating experiments with our *in vitro* model, such as hEPN time-courses or dose-response studies, could be performed to demonstrate the ability of hEPN to rescue Cat-D activity and to help more accurately place Cat-D within the hierarchy of Aβ-initiated cell death cascade, providing us with a critical, novel look at the molecular pathogenesis of this devastating neurodegenerative disease. Our Cat-D activity assay may also be applied to alternate experimental models, such as transgenic Alzheimer's mice similar to those used in this project's investigation of SOD, to measure Cat-D activity in more complicated biological systems. Since cultured neuronal cells are amenable to RNAi treatments, that technique could also be explored to knockdown expression of individual pathway components (Cat-D, caspase-3, caspase-2, caspase-9, caspase-12) (**Figure-17**) and determine which are essential for Aβ-induced cell death. With respect to ROS studies, enzymes other than SOD which help to alleviate ROS (such as catalase or glutathione

peroxidase) could also be monitored in our AD mice. Further, a TBARS assay could be used to determine whether cytoplasmic ROS actually declines with hEPN treatment, in correlation with our observed increases in SOD levels.

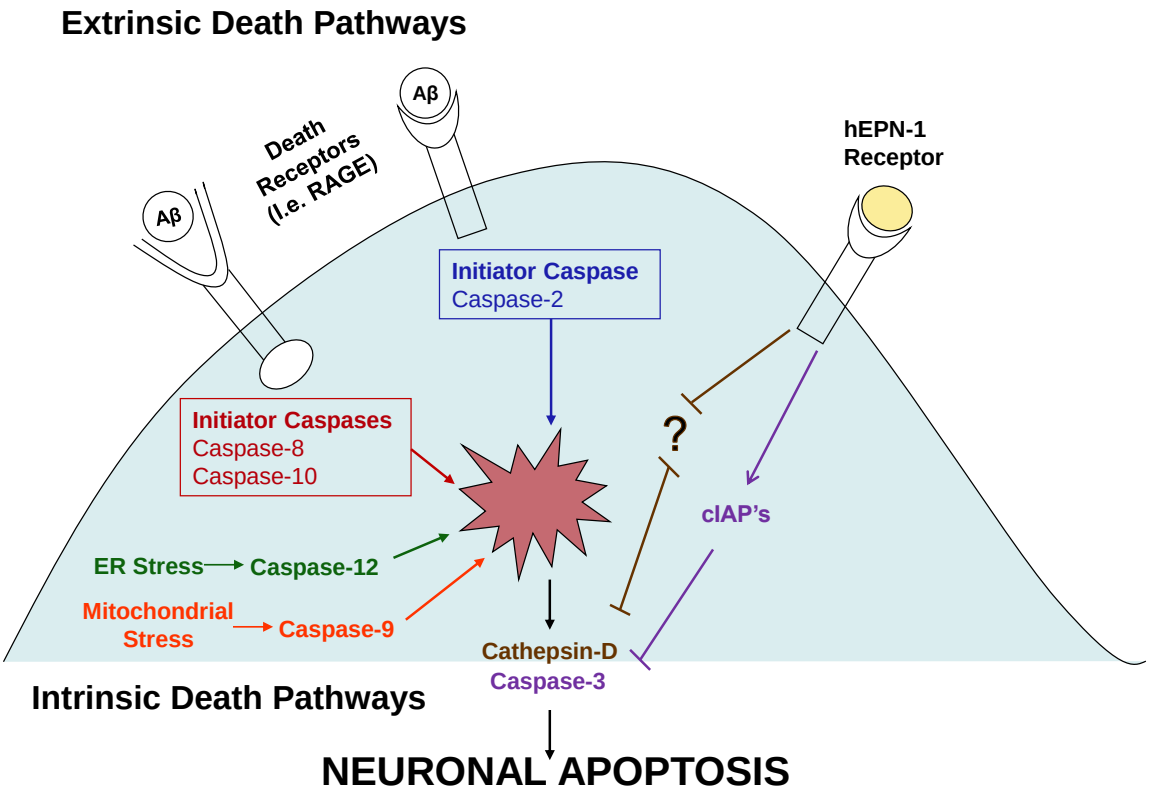

Figure-17: Diagram Summarizing Our Lab's Previous Work and our Hypothesized Role for Cat-D. Our lab previously demonstrated that treatment of cultured SHSY cells with Yankner peptide decreases cell survival (Stovall, 2006), increases Caspases-2 and -3 (Kapoor, 2007), and increases tau hyper-phosphorylation and TUNEL staining for DNA fragmentation (Ronayne, 2008), while treatment of cells with EPN increases cellular inhibitors of apoptosis (cIAPs) (Rawal, 2009), presumably using a different receptor. This project introduces the lysosomal aspartic protease cathepsin-D to the proposed death pathways of neuronal apoptosis, though its precise role and position within the hierarchy remain unidentified.

REFERENCES

Adams D, Shashoua V. (1994). Cloning and sequencing the genes encoding goldfish and carp ependymin. *Gene*, 141: 237-241.

Adams D, Kiyokawa M, Getman M, Shashoua V. (1996). Genes encoding giant danio and golden shiner ependymin. *Neurochemical Research*, 21: 377-384.

Adams DS, Hasson B, Boyer-Boiteau, A, El-Khishin A, Shashoua VE. (2003). A peptide fragment of ependymin neurotrophic factor uses protein kinase C and the mitogen activated protein kinase pathway to activate c-Jun N-terminal kinase and a functional AP-1 containing c-Jun and c-Fos proteins in mouse NB2a cells. *Journal of Neuroscience Research* 72: 405-416.

Allen RG, Tresini M. (2000). Oxidative stress and gene regulation. *Free Radical Biology and Medicine*, 28: 463-499.

Alzheimer's Association. (2010). 2010 Alzheimer's Disease Facts and Figures. *Alzheimer's & Dementia*, Volume 6. *http://www.alz.org/documents_custom/report_alzfactsfigures2010.pdf*

Alzheimer's Disease International. (2010. World Alzheimer's Report 2010: the global economic impact of dementia. *http://www.alz.co.uk/research/files/WorldAlzheimerReport 2010.pdf*

Alzheimer's Foundation of America (AFA). (2010). About Alzheimer's. Retrieved 15 February, 2011, from *http://www.alzfdn.org/AboutAlzheimers/definition.html*

Apostolopoulos J, Sparrow RL, McLeod JL, Collier FM, Darcy PK, Slater HR, Ngu C, Gregorio-King CC, Kirkland MA. (2001). Identification and characterization of a novel family of mammalian ependymin-related proteins (MERPs) in hematopoietic, nonhematopoietic, and malignant tissues. *DNA Cell Biology*, 20: 625-635.

Armstrong RA. (2006). Plaques and tangles and the pathogenesis of Alzheimer's disease. *Folia Neuropathologica*, 44 (1): 1-11.

Barinaga M. (1994). Neurotrophic factors enter the clinic. *Science*, 264: 772-774.

Benes P, Vetvicka V, Fusek M. (2008). Cathepsin D – many functions of one aspartic protease. *Critical Reviews in Oncology & Hematology*, 68(1): 12-28.

Benowitz LI, Shashoua VE. (1997). Localization of a brain protein metabolically linked with behavioral plasticity in the goldfish. *Brain Research*, 11 (2): 227-242.

Bidere N, Lorenzo HK, Carmona S, Laforge M, Harper F, Dumont C and Senik A. (2003). Cathepsin D Triggers Bax Activation, Resulting in Selective Apoptosis-inducing Factor (AIF) Relocation in T Lymphocytes Entering the Early Commitment Phase to Apoptosis. *J. Biol. Chem.*, 278, 31401–31411.

Blurton-Jones M, Kitazawa M, Martinez-Coria H, Castello NA, Müller FJ, Loring JF, Yamasaki TR, Poon WW, Green KN, LaFerla FM. (2009). Neural stem cells improve cognition via BDNF in a transgenic model of Alzheimer disease. *Proceedings of the National Academy of Science*, 106(32): 13594-13599. *www.ncbi.nlm.nih.gov/pubmed/19633196*

Carlson MC, Erickson KI, Kramer AF, Voss MW, Bolea N, Mielke M, McGill S, Rebok GW, Seeman T, Fried LP. (2009). Evidence for neurocognitive plasticity in at-risk older adults: the experience corps program. *Journals of Gerontology, Series A: Biological Sciences and Medical Sciences*, 64(12): 1275-1282. *www.ncbi.nlm.nih.gov/pubmed/19692672*

Cataldo AM, Barnett JL, Berman SA, Li J, Quarless S, Bursztajn S, Lippa C, Nixon RA. (1995). Gene expression and cellular content of cathepsin D in Alzheimer's disease brain: evidence for early up-regulation of the endosomal-lysosomal system. *Neuron*, 14(3): 671-680.

Chwieralski CE, Welte T, Buhling F. (2006). Cathepsin-regulated apoptosis. *Apoptosis*, 11(2): 143-149.

Clark CM, Schneider JA, Bedell BJ, Beach TG, Bilker WB, Mintun MA, Pontecorvo MJ, Hefti F, Carpenter AP, Flitter ML, Krautkramer MJ, Kung HF, Coleman RE, Doraiswamy PM, Fleisher AS, Sabbagh MN, Sadowsky CH, Reiman EM, Zehntner SP, Skovronsky DM. (2011). Use of florbetapir-PET for imaging β-amyloid pathology. *JAMA*, 305(3): 275-283. *http://jama.ama-assn.org/content/305/3/275.short*

Connor B, Dragunow M. (1998). The role of neuronal growth factors in neurodegenerative disorders of the human brain. *Brain Research Review* 27: 1-39.

Conus S, Perozzo R, Reinheckel T, Peters C, Scapozza L, Yousefi S, Simon H. (2008). Caspase-8 is activated by cathepsin D initiating neutrophil apoptosis during the resolution of inflammation. *JEM*, 205(3): 685-698.

Cooke JR, Ayalon L, Palmer BW, Loredo JS, Corey-Bloom J, Natarajan L, Liu L, Ancoli-Israel S. Sustained use of CPAP slows deterioration of cognition, sleep, and mood in patients with Alzheimer's disease and obstructive sleep apnea: a preliminary study. *Journal of Clinical Sleep Medicine* 2009; 5(4): 305-309. *www.ncbi.nlm.nih.gov/pubmed/19968005*

Dong Y, Zhang G, Zhang B, Moir RD, Xia W, Marcantonio ER, Culley DJ, Crosby G, Tanzi RE, Xie Z. (2009). The common inhalational anesthetic sevoflurane induces apoptosis and increases beta-amyloid protein levels. *Archives of Neurology*, 66(5):620-631. *www.ncbi.nlm.nih.gov/pubmed/19433662*

Ferrer I, Lopez E, Pozas E, Ballabriga J, Marti E. (1998). Multiple neurotrophic signals converge in surviving CA1 neurons of the gerbil hippocampus following transient forebrain ischemia. *Journal of Comparative Neurology* 394: 416-430.

Goedert M and Spillantini MG. (2006). A century of Alzheimer's disease. *Science*, 314: 777-781.

Guicciardi ME, Leist M, Gores GJ. (2004). Lysosomes in cell death. *Oncogene*, 23: 2881-2890.

Harold D, Abraham R, Hollingworth P, Sims R, Gerrish A, Hamshere ML, Pahwa JS, Moskvina V, Dowzell K, Williams A, Jones N, Thomas C, Stretton A, Morgan AR, Lovestone S, Powell J, Proitsi P, Lupton MK, Brayne C, Rubinsztein DC, Gill M, Lawlor B, Lynch A, Morgan K, Brown KS, Passmore PA, Craig D, McGuinness B, Todd S, Holmes C, Mann D, Smith AD, Love S, Kehoe PG, Hardy J, Mead S, Fox N, Rossor M, Collinge J, Maier W, Jessen F, Schürmann B, van den Bussche H, Heuser I, Kornhuber J, Wiltfang J, Dichgans M, Frölich L, Hampel H, Hüll M, Rujescu D, Goate AM, Kauwe JS, Cruchaga C, Nowotny P, Morris JC, Mayo K, Sleegers K, Bettens K, Engelborghs S, De Deyn PP, Van Broeckhoven C, Livingston G, Bass NJ, Gurling H, McQuillin A, Gwilliam R, Deloukas P, Al-Chalabi A, Shaw CE, Tsolaki M, Singleton AB, Guerreiro R, Mühleisen TW, Nöthen MM, Moebus S, Jöckel KH, Klopp N, Wichmann HE, Carrasquillo MM, Pankratz VS, Younkin SG, Holmans PA, O'Donovan M, Owen MJ, Williams J. (2009). Genome-wide association study identifies variants in CLU and PCALM associated with Alzheimer's disease. *Nature Genetics*, 41(10): 1088-1093. *www.ncbi.nlm.nih.gov/pubmed/19734902*

Hefti F. (1997). Pharmacology of neurotrophic factors. *Annual Review of Pharmacology and Toxicology*, 37: 239-267.

Heron MP, Hoyert DL, Xu J, Scott C, Tejada-Vera B. (2008). Deaths: preliminary data for 2006. *National Vital Statistics Report (CDC)*, 56(16). *http://www.cdc.gov/nchs/data/nvsr/nvsr56/nvsr56_16.pdf*

Johnson DK, Storandt M, Morris JC, Galvin JE. (2009). Longitudinal study of the transition from healthy aging to Alzheimer disease. Archives of Neurology, 66(10): 1254-1259. *www.ncbi.nlm.nih.gov/pubmed/19822781*

Kadish I, Thibault O, Blalock EM, Chen KC, Gant JC, Porter NM, Landfield PW. (2009). Hippocampal and cognitive aging across the lifespan: a bioenergetic shift precedes and increased cholesterol trafficking

parallels memory impairment. *Journal of Neuroscience*, 29(6): 1805-1916. www.ncbi.nlm.nih.gov/pubmed/19211887

Kang JE, Lim MM, Bateman RJ, Lee JJ, Smyth LP, Cirrito JR, Fujiki N, Nishino S, Holtzman DM. (2009). Amyloid-beta dynamics are regulated by orexin and the sleep-wake cycle. *Science*, 326(5955):1005-1007. (E-publication) www.ncbi.nlm.nih.gov/pubmed/19779148

Kim J, Castellano JM, Jiang H, Basak JM, Parsadanian M, Pham V, Mason SM, Paul SM, Holtzman DM. (2009). Overexpression of low-density lipoprotein receptor in the brain markedly inhibits amyloid deposition and increases extracellular A-beta clearance. *Neuron*, 64(5): 632-644. www.ncbi.nlm.nih.gov/pubmed/20005821

Leissring MA, Reinstatler L, Sahara T, Sevlever D, Roman R, Ji Z, Li L, Lu Q, Saftig P, Levites Y, Golde T, Burgess J, Ertekin-Taner N, Eckman E. (2009). Cathepsin D knockout mice harbor large and highly selective increases in cerevral AB42 and tau: implications for Alzheimer's disease pathogenesis. *Alzheimer's & Dementia*, 5(4 Supp): 155-156.

Lindsay R, Wiegand S, Altar C, DiStefano P. (1994). Neurotrophic factors: from molecule to man. *Trends in Neurosciences*, 17: 182-190.

Lu PH, Edland SD, Teng E, Tingus K, Petersen RC, Cummings JL. (2009). Donepezil delays progression to AD in MCI subjects with depressive symptoms. *Neurology*, 72(24): 2115-2121. www.ncbi.nlm.nih.gov/pubmed/19528519

Lu Y, Ansar S, Michaelis ML, Blagg BS. (2009). Neuroprotective activity and evaluation of Hsp90 inhibitors in an immortalized neuronal cell line. *Bioorganic & Medicinal Chemistry*, 17(4): 1709-1715. www.ncbi.nlm.nih.gov/pubmed/19138859

Luo W, Sun W, Taldone T, Rodina A, Chiosis G. (2010). Heat shock protein 90 in neurodegenerative diseases. *Molecular Neurodegeneration*, Jun 3; 5: 24. www.ncbi.nlm.nih.gov/pubmed/20525284

Mastroeni D, McKee A, Grover A, Rogers J, Coleman PD. (2009). Epigenetic differences in cortical neurons from a pair of monozygotic twins discordant for Alzheimer's disease. *PloS One*, 4(8):e6617. www.ncbi.nlm.nih.gov/pubmed/19672297

Mawuenyega KG, Sigurdson W, Ovod V, Munsell L, Kasten T, Morris JC, Yarasheski KE, and Bateman RJ. (2010). Decreased Clearance of CNS β-Amyloid in Alzheimer's Disease. *Science*, 330: 1774.

McCord JM, Keele Jr. BB, Fridovich I. (1971). The enzyme-based theory of obligate anaerobiosis: the physiological function of superoxide dismutase. *Proc. Nat. Acad. Sci., 68(5): 1024-1027.*

Nagahara AH, Merrill DA, Coppola G, Tsukada S, Schroeder BE, Shaked GM, Wang L, Blesch A, Kim A, Conner JM, Rockenstein E, Chao MV, Koo EH, Geschwind D, Masliah E, Chiba AA, Tuszynski MH. (2009). Neuroprotective effects of brain-derived neurotrophic factor in rodent and primate models of Alzheimer's disease. *Nature Medicine*, 15(3):331-337. www.ncbi.nlm.nih.gov/pubmed/19198615

Orr WC, Sohal RS. (1994). Extension of life-span by overexpression of superoxide dismutase and catalase in Drosophila melangaster. *Science*, 263: 1128-1131.

Papassotiropoulos A, Bagli M, Feder O, Jessen F, Maier W, Luise R, Ludwig M, Schwab SG, Heun R. (1999). Genetic polymorphism of cathepsin D is strongly associated with the risk for developing sporadic Alzheimer's disease. *Neuroscience Letters*, 262(3): 171-174.

Parikh S. (2003). Ependymin peptide mimetics that assuage ischemic damage increase gene expression of the anti-oxidative enzymes SOD. WPI Master's Thesis, April, 2003.

Petanceska S, Ryan L, Silverberg N, Buckholtz N. (2009). Commentary on "a roadmap for the prevention of dementia II. Leon Thal Symposium 2008." Alzheimer's disease translational research programs at the National Institute on Aging. *Alzheimer's & Dementia*, 5(2):130-132. www.ncbi.nlm.nih.gov/pubmed/19328442

Progress Report on Alzheimer's Disease: translating new knowledge. (2009). U.S. Department of Health and Human Services, National Institutes of Health, National Institute of Aging. NIH Publication Number: 10-7500.

Puzzo D, Staniszewski A, Deng SX, Privitera L, Leznik E, Liu S, Zhang H, Feng Y, Palmeri A, Landry DW, Arancio O. (2009). Phosphodiesterase 5 inhibition improves synaptic function, memory, and amyloid-beta load in an Alzheimer's disease mouse model. *Journal of Neuroscience*, 29(25):8075-8086. www.ncbi.nlm.nih.gov/pubmed/19553447

Qiao L, Hamamichi S, Caldwell KA, Caldwell GA, Yacoubian TA, Wilson S, Xie Z, Speake LD, Parks R, Crabtree D, Liang Q, Crimmins S, Schneider L, Uchiyama Y, Iwatsubo T, Zhou Y, Peng L, Lu Y, Standaert DG, Walls KC, Shacka JJ, Roth KA, Zhang J. (2008). Lysosomal enzyme cathepsin D protects against alpha-synuclein aggregation and toxicity. *Molecular Brain*, 1: 17.

Rapoport M, Dawson HN, Binder LI, Vitek MP, Ferreira A. (2002). Tau is essential to β-amyloid-induced neurotoxicity. *PNAS*, 99(9): 6364-6369.

Reiman EM, Chen K, Liu X, Bandy D, Yu M, Lee W, Ayutyanont N, Keppler J, Reeder SA, Langbaum JB, Alexander GE, Klunk WE, Mathis CA, Price JC, Aizenstein HJ, DeKosky ST, Caselli RJ. (2009). Fibrillar amyloid-beta burden in cognitively normal people at 3 levels of genetic risk for Alzheimer's disease. *Proceedings of the National Academy of Sciences*, 106(16):6820-6825. www.ncbi.nlm.nih.gov/pubmed/19346482

Roberson ED & Mucke L. (2006). 100 years and counting: prospects for defeating Alzheimer's Disease. *Science*, 314: 781-784.

Roberson ED, Scearce-Levie K, Palop JJ, Yan F, Cheng IH, Wu T, Gerstein H, Yu G, and Mucke L. (2007). Reducing Endogenous Tau Ameliorates Amyloid-β-Induced Deficits in an Alzheimer's Disease Mouse Model. *Science* 316: 750-754.

Saif S. (2004). AP-1 is required for CMX-8933-induced SOD upregulation, and is translocated in response to human EPN mimetic. WPI Thesis, April 2004.

Sampei K, Mandir AS, Asano Y, Wong PC, Traystman RJ, Dawson VL, Dawson TM, Hurn PD. (2000). Stroke outcome in double-mutant antioxidant transgenic mice. *Stroke*, 31: 2685-2691.

Sanders L. (2011). Memories Can't Wait: researchers rethink the role of amyloid in causing Alzheimer's. *ScienceNews*, 179(6): 24.

Schneider JA, Aggarwal NT, Barnes L, Boyle P, Bennett DA. (2009). The neuropathology of older persons with and without dementia from community versus clinic cohorts. *Journal of Alzheimer's Disease*, 18(3): 691-701. www.ncbi.nlm.nih.gov/pubmed/19749406

Shashoua V, Adams D, Boyer-Boiteau A, Cornell-Bell A, Li F, Fisher M. (2003). Neuro-protective effects of a new synthetic peptide (CMX-9236) in in vitro and in vivo models of cerebral ischemia. *Brain Research*, 963: 214-223.

Shen L, Figurov A, Lu B. (1997). Recent progress in studies of neurotrophic factors and their clinical applications. *Journal of Molecular Medicine*, 75: 637-644.

Sheng H, Brady T, Pearlstein R, Crapo J, Warner D. (1999). Extracellular superoxide dismutase deficiency worsens outcome from fetal focal cerebral ischemia in the mouse. *Neuroscience Letters*, 267: 13-16.

Schuur M, Ikram MA, van Swieten JC, Isaacs A, Vergeer-Drop JM, Hofman A, Ostra BA, Breteler MMB, van Duijn CM. (2009). Cathepsin D gene and the risk of Alzheimer's disease: a population-based study and meta-analysis. *Neurology of Aging*, November 18 (ePub).

Smith GE, Housen P, Yaffe K, Ruff R, Kennison RF, Mahncke HW, Zelinski EM. (2009). A cognitive training program based on principles of brain plasticity: results from the Improvement in Memory with

Plasticity-based Adaptive Cognitive Training (IMPACT) study. *Journal of the American Geriatrics Society*, 57(4): 594-603.

Snitz BE, O'Meara ES, Carlson MC, Arnold AM, Ives DG, Rapp SR, Saxton J, Lopez OL, Dunn LO, Sink KM, DeKosky ST. Ginkgo biloba for preventing cognitive decline in older adults: a randomized trial. *Journal of the American Medical Association* 2009; 302(24):2663-2670. *www.ncbi.nlm.nih.gov/pubmed/20040554*

Sonnen JA, Larson EB, Brickell K, Crane PK, Woltjer R, Montine TJ, Craft S. (2009). Different patterns of cerebral injury in dementia with or without diabetes. *Archives of Neurology*, 66(3):315-322. *www.ncbi.nlm.nih.gov/pubmed/19139294*

Stovall K. 2006. Partial restoration of cell survival by a human ependymin mimetic in an *in vitro* Alzheimer's disease model. WPI Master's Thesis, August, 2006.

Takahashi RH, Capetillo-Zarate E, Lin MT, Milner TA, Gouras GK. (2008). Co-occurrence of Alzheimer's disease β-amyloid and tau pathologies at synapses. *Neurobiology and Aging*, 31: 1145-1152.

Tuszynski M, Gage F. (1994). Neurotrophic factors and diseases and the nervous system. *Annals of Neurology*, 35: S9-S12.

Vancompernolle K, Van Herreweghe F, Pynaert G, Van de Craen M, De Vos K, Totty N, Sterling A, Fiers W, Vandenabeele P and Grooten J. (1998). Atractyloside-induced release of cathepsin B, a protease with caspase-processing activity. *FEBS Lett.*, 438, 150–158.

Vas CJ, Rajkumar S, Tanyakitpisal P, Chandra V. (2001). Alzheimer's Disease: the brain killer. *World Health Organization*. *http://www.searo.who.int/LinkFiles/Health_and_Behaviour_alzheimers.pdf*

Venarucci D, Venarucci V, Vallese A, Battila L, Casado A, De la Torre R, Lopez-Fernandez ME. (1999). Free radicals: important cause of pathologies related to ageing. *Panminerva Medicine* 4: 335-339.

Verdile G, Fuller S, Atwood CS, Laws SM, Gandy SE, Martins RN. (2004). The role of beta-amyloid in Alzheimer's disease: still a cause of everything or the only one who got caught? *Pharmacological Research*, 50: 397-409.

Walsh DM, Klyubin I, Fadeeva JV, Cullen WK, Anwyl R, Wolfe MS, Rowan MJ, Selkoe DJ. (2002). Naturally secreted oligomers of amyloid β protein potently inhibit hippocampal long-term potentiation *in vivo*. *Nature*, 416: 535-539.

Wilson RS, Arnold SE, Schneider JA, Boyle PA, Buchman AS, Bennett DA. (2009). Olfactory impairment in presymptomatic Alzheimer's disease. Annals of the New York Academy of Sciences, 1170: 730-735. *www.ncbi.nlm.nih.gov/pubmed/19506226*

Yaffe K, Weston A, Graff-Radford NR, Satterfield S, Simonsick EM, Younkin SG, Younkin LH, Kuller L, Ayonayon HN, Ding J, Harris TB. (2011). Association of plasma β-amyloid level and cognitive reserve with subsequent cognitive decline. *JAMA*, 305(3): 261-266. *http://jama.ama-assn.org/content/305/3/261.short*

Yan SD, Chen X., Fu J, Chen M, Zhu H, Roher A, Slattery T, Zhao L, Nagazhima M, Morser J, Mighelo A, Nawroth P, Stern D, Schmidt AM. (1996). RAGE and amyloid-β peptide neurotoxicity in Alzheimer's disease. *Nature*, 382: 685-691.

Yao J, Irwin RW, Zhao L, Nilson J, Hamilton RT, Brinton RD. (2009). Mitochondrial bioenergetic deficit precedes Alzheimer's pathology in female mouse model of Alzheimer's disease. *Proceedings of the National Academy of Sciences*, 106(34): 14670-14675.

Yu D, Silva GA. (2008). Stem cell sources and therapeutic approaches for central nervous system and neural retinal disorders. *Neurosurgical Focus*, 24 (3-4): 1-23.

Yuan J, Yankner BA. (2000). Apoptosis in the nervous system. *Nature*, 407: 802-809.

Zuccato C, Cattaneo E. (2009). Brain-derived neurotrophic factor in neurodegenerative diseases. *Nature Reviews Neurology*, 5: 311-322.

Zhao M, Antunes F, Eaton JW, Brunk UT. (2003). Lysosomal enzymes promote mitochondrial oxidant production, cytochrome c release and apoptosis. *Eur. J. Biochem.*, 270, 3778–3786.

Zheng H, Koo EH. (2006). The amyloid precursor protein: beyond amyloid. *Molecular Neurodegeneration*, 1(5): 1-12.